



**HAL**  
open science

## Coal ash for removing toxic metals and phenolic contaminants from wastewater: A brief review

Abdelkader Labidi, Haitao Ren, Atif Sial, Hui Wang, Eric Lichtfouse, Chuanyi Wang

### ► To cite this version:

Abdelkader Labidi, Haitao Ren, Atif Sial, Hui Wang, Eric Lichtfouse, et al.. Coal ash for removing toxic metals and phenolic contaminants from wastewater: A brief review. *Critical Reviews in Environmental Science and Technology*, 2023, 53, pp.2006 - 2029. 10.1080/10643389.2023.2206781 . hal-04229023

**HAL Id: hal-04229023**

**<https://hal.science/hal-04229023>**

Submitted on 5 Oct 2023

**HAL** is a multi-disciplinary open access archive for the deposit and dissemination of scientific research documents, whether they are published or not. The documents may come from teaching and research institutions in France or abroad, or from public or private research centers.

L'archive ouverte pluridisciplinaire **HAL**, est destinée au dépôt et à la diffusion de documents scientifiques de niveau recherche, publiés ou non, émanant des établissements d'enseignement et de recherche français ou étrangers, des laboratoires publics ou privés.

Critical Reviews in Environmental Science and Technology 23, 2006-2029, 2023  
<https://doi.org/10.1080/10643389.2023.2206781>

## **Coal ash for removing toxic metals and phenolic contaminants from wastewater: A brief review**

**Abdelkader Labidi, Haitao Ren, Atif Sial, Hui Wang, Eric Lichtfouse & Chuanyi Wang**

# Coal ash for removing toxic metals and phenolic contaminants from wastewater: A brief review

Abdelkader Labidi<sup>a</sup>, Haitao Ren<sup>a</sup>, Atif Sial<sup>a</sup>, Hui Wang<sup>a</sup>, Eric Lichtfouse<sup>b</sup>   
and Chuanyi Wang<sup>a</sup>

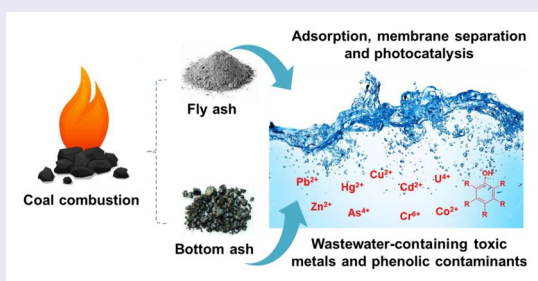
<sup>a</sup>School of Environmental Science and Engineering, Shaanxi University of Science and Technology, Xi'an, PR China;

<sup>b</sup>CNRS, IRD, INRAE, CEREGE, Aix Marseille Univ, Aix en Provence, France

## ABSTRACT

Over the past few years, population growth, industrial progress and climate change have led to water scarcity. Thus, water pollution caused by hazardous soluble and insoluble pollutants, such as toxic metals and phenolic compounds, has become an important problem that should be dealt with urgently. For instance, new methods have been introduced to convert low-cost raw materials (i.e. coal fly ash and coal bottom ash “wastes-to-resource”) into suitable materials for new cleaner production to achieve sustainability

goals in wastewater-containing toxic metals and phenolic compounds purification. Obviously, the functionalization of coal fly ash and bottom ash enhances the ability of coal ash-based entities as potential materials in wastewater remediation technologies. Here, we review the application of coal ashes, including coal bottom ash and fly ash-based materials for toxic metals and phenolic compounds removal. We also examine their structural properties and functionalization to enhance their affinities toward these pollutants in aqueous environment. Even though each process has its own benefits and limitations, coal ash-based materials appear promising for the removal of toxic metals and phenolic compounds using adsorption, membrane filtration, and photocatalysis. Overall, the study on the availability of coal fly ash and bottom ash for wastewater treatment have resulted in high removal efficiencies for toxic metals and phenolic compounds. In the future, new recycling methods for coal ashes as new water purification agents should be further studied and advanced processes should be investigated in order to achieve wastewater remediation purposes.



**KEYWORDS** Coal bottom ash; coal fly ash; low-cost raw materials; toxic metals; phenolic compounds; wastewater

**HANDLING EDITORS** Esther Álvarez-Ayuso and Lena Q. Ma

## 1. Introduction

Water is an essential element for humans, animals and plants (Alawi et al., 2022; Iqbal et al., 2022; Tu et al., 2022). Water also plays an important role in many fields, particularly the industrial and agricultural sectors (Ferreira et al., 2022; Li, Huang, et al., 2022). Nowadays, water resources face issues of contamination by pollutants such as organic, inorganic, microbial, fertilizer and radioactive substances resulting from urbanization, modernization and dying industries (Bing et al., 2022; Gangani et al., 2022; Li, Zhang, et al., 2022; Picetti et al., 2022; Zhou et al.,

2021). Consequently, the preservation of water is becoming a great concern to avoid the harmful impacts of water pollution on soil, human health and the whole ecosystem (Liu et al., 2021; Loi et al., 2022; Some et al., 2021). This issue has been given the great interest by scientists and researchers (Tiller et al., 2021; Wang, Zhang, et al., 2022).

Recently, reports on residues removal from water and soil have evidenced that toxic metals can be considered as the top-list inorganic pollutants of water (Hasan et al., 2022; Helmrich et al., 2022; Li, Liu, et al., 2022; Luo et al., 2022; Zamora-Ledezma et al., 2021). Although some metals, for example, calcium (Ca), magnesium (Mn), zinc (Zn), iron (Fe), copper (Cu), and nickel (Ni), are necessary micronutrients in our body, they can be toxic for humans, plants and animals when taken up in high concentrations or in certain forms (Ayub et al., 2021; Glasner et al., 2021). Other toxic metals such as chromium (Cr), arsenic (As), cadmium (Cd), lead (Pb), and mercury (Hg) are classified as poisonous compounds for humans even at low concentrations (Mukherjee et al., 2022; Sun et al., 2022). The main sources of heavy metals are fossil fuel combustion, metallurgical and agricultural production, mining, and industrial sectors, waste disposition as well as biomass combustion and coal burning for winter heating (Cui et al., 2022; Mukherjee et al., 2022; Sun et al., 2022). The bio-accumulation of toxic metals in plants and their discharge in water cause various illnesses like Parkinson's diseases including olfactory dysfunction, constipation, sleeping disorder, tremor, rigidity, and bradykinesia (Vellingiri et al., 2022). In addition, the contamination of water with heavy metals may lead to cardiovascular diseases, renal, and urological diseases (Guo et al., 2022; Korashy et al., 2017).

Phenolic compounds are water-soluble organic pollutants with an aromatic ring bearing one or more hydroxyl groups (Hashim, Fen, Omar, Fauzi, & Daniyal, 2021). They can be classified into various types including flavonoids, hydroquinone, polymeric phenolic compounds, for example, tannin and lignin, phenolic acids, for example, benzoic acid and cinnamic acid, simple phenols, pyrocatechol, and resorcinol. Phenolic compounds are widely used in industry, agriculture, cosmetics, food production, petroleum processing and medicines (Dalanta & Kusworo, 2022; Hashim, Fen, Omar, Fauzi, & Daniyal, 2021; Lei et al., 2021; Omar et al., 2022; Xu et al., 2022). Besides, water contamination by phenolic compounds such as phenol, 2-chlorophenol, 2,4-dichlorophenol, nitrophenol and bisphenol induce estrogenic disorders in aquatic wildlife (Hashim, Fen, Omar, & Fauzi, 2021; Ramos et al., 2021).

Techniques to remediate waters contaminated with toxic metals and phenolic compounds include adsorption, membrane filtration, microbial degradation, flocculation, chemical oxidation, and UV light degradation (Bi et al., 2022; Cheng et al., 2022; Joshi & Gururani, 2022; Rajendran et al., 2022; Ramos et al., 2022; Said et al., 2022; Sharma, Pap, et al., 2022; Wang, Yang, et al., 2022; Wu & Ke, 2022; Yavari-Bafghi et al., 2022). Microbial degradation and flocculation techniques have been widely employed to remove, treat and detect toxic metals and phenolic contaminants in wastewater due to their low-cost implementation (Cheng et al., 2022; Yavari-Bafghi et al., 2022). However, chemical oxidation has been considered the least attractive technique for toxic metals and phenolic compounds remediation due to its expensive cost and short lifetime (Wu & Ke, 2022). For the same purpose, photodegradation process has been applied for toxic metals and phenolic contaminants degradation owing to its green and eco-friendly characters as well as its ability to reduce completely these pollutants in some cases (Sharma, Pap, et al., 2022). On the other hand, when applied for wastewater remediation this process suffers from many disadvantages such as the inability of some selected photocatalysts to utilize solar light as the source of UV light, the hard catalysts separation and the stability of catalytic materials and pH conditions (Sharma, Pap, et al., 2022). As a solution, many researchers have given particular attention to membrane separation which is a more efficient and sustainable process of wastewater purification, compared to the traditional treatment systems (Ramos et al., 2022; Said et al., 2022). Moreover, adsorption process is classified as one of the most successful approaches for toxic metals and phenolic contaminants removal due to its low-cost installation and high efficiency in removing these emerging contaminants (Rajendran et al., 2022; Wang, Yang, et al., 2022). For adsorption, raw cellulose has been converted into cellulose nanofibers and nanocrystals with

high surface area (Ray & Iroegbu, 2021). Cellulose and nano-cellulosic derivatives are ranked at the top list of the biomaterials intensively used in water and wastewater remediation (Ajala et al., 2022). Cellulosic materials are abundant in nature and can be obtained from several biomass resources such as woody biomass, bacteria and algae (Ajala et al., 2022). The cellulose is generally used as a natural support to design new adsorbents because of its high reactivity, which ensures its physicochemical modification, its low-cost and its easy transformation into commercial products which can be utilized in wastewater treatment technologies (Ajala et al., 2022). It can be also employed as raw material and can be functionalized by several organic and inorganic reagents to enhance its adsorptive proprieties and consequently improve its adsorption capacity toward organic and inorganic pollutants (Ray & Iroegbu, 2021). Other natural polymers, such as chitin, a polysaccharide, and chitosan, have been explored for wastewater decontamination (Picos-Corrales et al., 2020). They are characterized by their high performances in removing suspended solids from wastewater (Keshvardoostchokami et al., 2021; Labidi et al., 2020; Salam et al., 2021). Surface modification of chitin and chitosan with organic and inorganic groups enhances adsorption and displays the versatility in chitin and chitosan composites for effective removal processes (Keshvardoostchokami et al., 2021; Picos-Corrales et al., 2020). Other natural polysaccharides have been utilized for wastewater remediation include starch, pectin, gum, and alginate (Akinterinwa et al., 2022; Giri & Badwaik, 2022; Li, Yang, et al., 2022; Shen et al., 2022; Soury et al., 2022).

Inorganic materials comprising zeolites, silica, clay, diatomite and metal oxides are also used in wastewater treatment (Abidin et al., 2021; Du et al., 2022; Jabbar et al., 2022; Mo et al., 2022; Taranu et al., 2022). Physical and chemical modification of inorganic materials has also improved wastewater remediation by adsorption, coagulation, electrochemistry, photo-electrochemistry and biological methods (Du et al., 2022; Mo et al., 2022; Pu et al., 2022; Taranu et al., 2022). Coal ash, including coal fly ash and coal bottom ash, are intensively used for silica, alumina and zeolite synthesis, building materials production and gas sensors (Gao & Iliuta, 2022; Meesala et al., 2020; Valeev et al., 2022). Here, we review the application of coal ash inorganic materials to separate and pre-concentrate toxic metals and phenolic compounds in wastewater. Besides, this review covers the preparation, the properties and the applications of coal fly ash and bottom in many physical forms, that is, powders, membranes, gels, films, nanocomposites, and magnetic particles for toxic metals and phenolic compounds decontamination. It also describes the chemical routes for the synthesis of coal ash-based materials and their characterization techniques. Additionally, the interactions of coal ash-based entities with toxic metals and phenolic compounds were examined. Then, the selective removal of these pollutants by adsorption, membrane filtration and photodegradation-reduction are described. The benefits and limitations of remediation processes are also outlined. The main objectives of this brief review are to prove that the coal ash-based entities are low-cost raw materials that can be utilized through commonly- practiced processes for wastewater containing toxic metals and phenolic compounds remediation. Adsorbents, membranes and photocatalysts are synthesized by adapting several preparation methods in order to improve the physicochemical proprieties of pure coal ashes. Consequently, the incorporation of such inorganic and organic groups on the coal ash surface makes these by-products as efficient and high selective materials for toxic metals and phenolic compounds removal from contaminated water.

## **2. Coal fly ash and bottom ash inorganic materials**

### **2.1. Coal fly ash**

#### **2.1.1. Production and classes of coal fly ash**

In 2018, Pacific Asia was the first producer of coal ash with annual production of more than 5000 million tonnes (65 wt. % in China). It was followed by North America, producing annually more than 500 million tonnes (91 wt. % in the United States) and less than 500 million tonnes

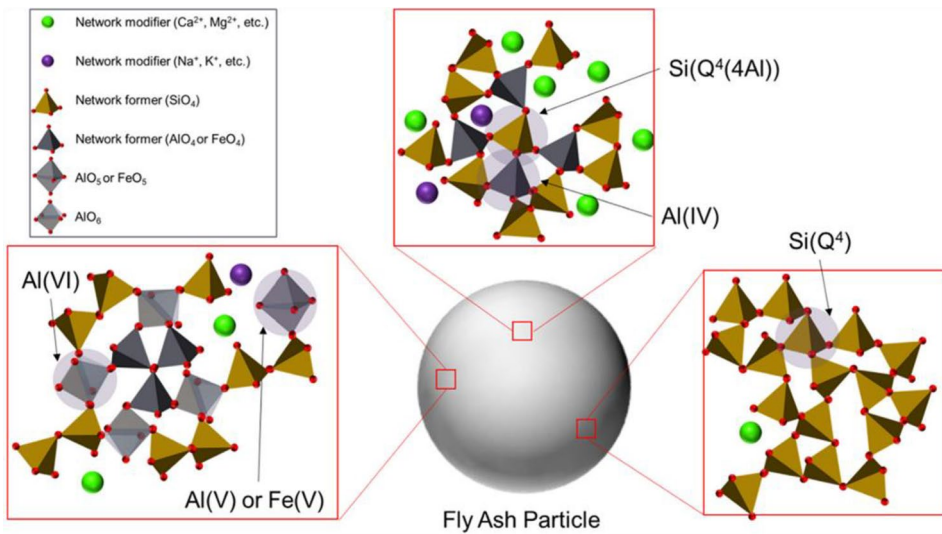


**Figure 1.** Schematic illustration of the glass structure in fly ash. Reprinted with permission of Elsevier from Jin et al. (2020).

**Table 1.** Physicochemical proprieties of coal fly ash and bottom ash.

Materials	Mineralogical compositions	Chemical compositions	Physical properties	Classes	References
Coal fly ash	Quartz, Mullite, Hematite, Melite and Merwinite	SiO <sub>2</sub> , Al <sub>2</sub> O <sub>3</sub> , Fe <sub>2</sub> O <sub>3</sub> , SiO <sub>2</sub> , TiO <sub>2</sub> , Na <sub>2</sub> O, Fe <sub>2</sub> O <sub>3</sub> , CaO, K <sub>2</sub> O, MgO, unburnt carbon (7.5 wt. %), trace metals	Diameter size range from 1.0 to 5.0 μm, specific gravities range from 1.6 to 3.1, pH values range from 1.2 to 12.5.	Class F and C	Alterary and Marei, (2021) and Zierold and Odoh (2020)
Coal bottom ash	Mullite, Magnetite, Meldspar, Quartz, Bituminous, Sub-bituminous, Anthracite and Lignite	SiO <sub>2</sub> , CaO, Al <sub>2</sub> O <sub>3</sub> , Na <sub>2</sub> O, MgO, Fe <sub>2</sub> O <sub>3</sub> , K <sub>2</sub> O, unburnt carbon (10 wt. %), trace metals	Specific surface range 1164–9849 m <sup>2</sup> g <sup>-1</sup> , particle size distributions range from 0.075 to 20 mm, pH values from 6.5 to more than 8.5.	Class F and C	Rashidi and Yusup (2016)

in Europe (25 wt.% in Hungary) (Alterary & Marei, 2021) (Supporting Information Figure S1). Coal fly ash, sometimes called fly ash, is the major product of coal combustion (70 wt. %) (Rashidi & Yusup, 2016). Coal fly ash collected from electrostatic precipitators contains trace metals, mineral constituents and unburnt carbon (7.5 wt. %) (Alterary & Marei, 2021; Rashidi & Yusup, 2016). Trace metals in fly ash can be divided into three classes (class I, II, and III) depending on the trace constituent elements, and the relative enrichment factor (RE) was calculated using the following Equation (1), (Zierold & Odoh, 2020):

$$RE = \frac{\text{Concentration of element in ash} * \text{Ash percentage in feed coal}}{\text{Concentration of element in coal} * 100} \quad (1)$$

The first class (class I) includes the nonvolatile elements, for example, aluminum, calcium, iron and magnesium of with a relative enrichment factor  $RE = 1.0$ . The second class (class II) encompasses trace metals such as cobalt, copper, nickel, chromium, manganese, barium, rubidium, beryllium, arsenic, cadmium, lead and zinc with a relative enrichment  $RE < 0.7$ . The third class (class III) contains chlorine, fluorine, mercury and selenium with relative enrichment  $RE \ll 1.0$ . Moreover, FA was classified into two main groups class C and class F fly ash (Alterary

& Marei, 2021). Class C ashes are pozzolanic, and cementitious produced from sub-bituminous or lignite coal burning. In this class, the amount of  $\text{Fe}_2\text{O}_3$ ,  $\text{Al}_2\text{O}_3$ , and  $\text{SiO}_2$  must be greater than 50%. Class F fly ash is pozzolanic brought out from either anthracite or bituminous burning of coal. In this class, the total amount of  $\text{SiO}_2$ ,  $\text{Al}_2\text{O}_3$ , and  $\text{Fe}_2\text{O}_3$  must be greater than 70% (Alterary & Marei, 2021). Coal fly ash is also classified according to pH in alkaline, neutral and acidic fly ash (Zierold & Odoh, 2020).

### **2.1.2. Physicochemical proprieties of coal fly ash**

The generated coal fly ash, a by-product obtained from coal combustion, is collected by electrostatic separators before its discharge into the atmosphere (Jin et al., 2020). Coal fly ash contains circular amorphous particles with a diameter size range in size within 1.0–5.0  $\mu\text{m}$  and crystalline phase accounts for to 50 wt.% of its mass (Table 1). Fly ash encompasses the following compounds: silicon dioxide ( $\text{SiO}_2$ ), aluminum oxide ( $\text{Al}_2\text{O}_3$ ), melite, and merwinite are related to (MgO) content and a little amount of  $\text{TiO}_2$ ,  $\text{Na}_2\text{O}$ ,  $\text{Fe}_2\text{O}_3$ ,  $\text{CaO}$ , and  $\text{K}_2\text{O}$  (Figure 1), unburnt carbon (7.5 wt.%) and heavy metals at trace levels such as cadmium (Cd), zinc (Zn), arsenic (As), mercury (Hg) and lead (Pb) (Jin et al., 2020; Wang et al., 2020; 2021). The presence of these crystalline/amorphous phases and the above mentioned elements in fly ash, give this low-cost raw material the following proprieties: specific surface area, small size, silt and clay-sized particles, adsorption capacity, low bulk density and higher water-holding capacity (Figure S2) (Cho et al., 2019; Jin et al., 2020; Wang et al., 2021).

## **2.2. Coal bottom ash**

### **2.2.1. Production and classes of coal bottom ash**

Coal bottom ash, also known as bottom ash, is the second product obtained from coal combustion (30 wt.%), less than coal fly ash (70 wt.%) (Rashidi & Yusup, 2016). Additionally, the world production of coal bottom ash was estimated to be 730 million tonnes (Singh et al., 2020), with Asian countries share exceeding 66 wt.%, followed by European and American countries (less than 40 wt.%) (Singh et al., 2020). In fact, there are four types of coal: bituminous, sub-bituminous, anthracite, lignite. Coal bottom ash can be classified into two major categories and can be described as a class F and class C (Rashidi & Yusup, 2016). Those belonging to the first class are materials containing high amount of silicon dioxide  $\text{SiO}_2$ , aluminum oxide  $\text{Al}_2\text{O}_3$ , ferric oxide  $\text{Fe}_2\text{O}_3$  (> 70 wt.%) and low amount of calcium oxide (CaO) (Table 1). However, class C encompasses bottom ash with high quantity of calcium oxide CaO and an amount of  $\text{SiO}_2$ ,  $\text{Al}_2\text{O}_3$ , and  $\text{Fe}_2\text{O}_3$  ranging from 50 to 70 wt.% (Rashidi & Yusup, 2016).

### **2.2.2. Physicochemical proprieties of coal bottom ash**

In general, coal bottom ash contains unburnt carbon (approximately 10 wt. %) and other elements such as  $\text{SiO}_2$ ,  $\text{Al}_2\text{O}_3$ ,  $\text{Fe}_2\text{O}_3$ ,  $\text{CaO}$ ,  $\text{K}_2\text{O}$ ,  $\text{Na}_2\text{O}$ , MgO, trace metals, and so on (Table 1, Rashidi & Yusup, 2016). Thus, it is highly amorphous with the presence of crystalline phases like mullite, magnetite, feldspar, and quartz. Furthermore, the presence of higher silica content makes coal bottom ash hydrophilic in nature (Singh et al., 2020). Moreover, the particles of coal bottom ash are mostly angular and irregular in shape with visible apertures, specific surface range of 1164–9849  $\text{m}^2 \text{g}^{-1}$  (Table 1), with specific gravity and fineness modulus of coal bottom ash varying between 1.20 and 2.47 and from 1.39 to 2.88, respectively (Rashidi & Yusup, 2016; Singh et al., 2020).

## **2.3. Applications of coal fly ash and bottom ash**

For years, fly ash has been applied as cementitious material (SCM) for brick and concrete industries, embankment and mine fill, ceramic fabrication, soil amelioration by neutralizing soil acidity, extraction of plant-available nutrients, eco-friendly catalysts, low-cost material for zeolites

**Table 2.** Industrial and environmental applications of coal fly ash and bottom ash.

Materials	Applications	References
Fly ash	Production and proprieties of fly ash.	Meesala et al. (2020)
Coal fly ash	Applications of fly ash to produce Portland cement concrete. Discussion about the extraction and synthesis methods of coal fly ash	Ju et al. (2021)
Coal fly ash	Evaluation of geometry, structural proprieties and performance of coal fly ash in porous materials synthesis. Annual coal fly ash accumulation rates, stored volumes and its chemical composition.	Valeev et al. (2022)
Coal fly ash and other solid wastes	Application of acid methods using coal fly ash for alumina production. Future research directions in the use of coal fly ash in aluminum industry.	Gao and Iliuta (2022)
Coal-based bottom ash	Pre-treatment of coal fly ash for zeolites, mesoporous silica, and silica aerogel synthesis. The application of coal fly ash as silica and/or alumina sources. The application of coal fly ash-based nanomaterials for capturing CO <sub>2</sub> and rare earth metal ions.	Rashidi and Yusup (2016)
Coal bottom ash	Production and disposal of bottom ash. Physicochemical proprieties of coal bottom ash. Conversion and application of bottom ash for zeolites synthesis and dyes removal.	Singh et al. (2020)
Coal fired power plant bottom ash and fly ash	Portland cement fabrication using coal bottom ash as additive. Performance of concretes based on coal bottom ash. Mechanical, durability and benefits of the obtained concretes. Reuses of coal ash including coal fly ash and coal bottom ash. Coal ash waste products for road construction, cement production, embankments, and construction materials.	Jayaranjan et al. (2014)

and magnetic spheres synthesis (Table 2), excellent remediants for gas sensors and aqueous residues in wastewater (Fu et al., 2022; Jain & Tembhurkar, 2022; Li et al., 2021; Sanna et al., 2022; Sharma, Kashyap, et al., 2022; Tan et al., 2022; Wang, Jin, et al., 2022; Wang et al., 2021; Zhang, Shi, et al., 2021) (Figure S3). In the last decade, the number of publications focusing on fly ash uses, higher than coal bottom ash, has increased from less than 500 publications in 2000 to more than 2000 publications in 2019 (Figure S4) (Alterary & Marei, 2021). Regardless of the application of coal bottom ash, the chemical compositions and the important thermal and mechanical characteristics of this inorganic material make it a potential waste to reuse in industrial and environmental domains (Table 2). Moreover, bottom ash has been applied in various fields of application such as cementitious material and concrete production, wastewater treatment, zeolite production, silica synthesis and gas capture (Mangi et al., 2018; Rashidi & Yusup, 2016; Singh et al., 2020).

For instance, recycling and changing the properties of coal fly ash and bottom ash by introducing organic and inorganic entities on their surfaces have been established them as effective remediants for several pollutants decontamination such as toxic metals and phenolic compounds. Thus, the transformation of coal ashes into zeolite materials, the treated coal ashes and their direct functionalization or transformation into a porous membrane, adsorbents and photocatalysts can be considered as a new alternative in materials synthesis and wastewater remediation technologies.

### 3. Coal ash adsorbents for contaminants remediation

#### 3.1. Removal of toxic metals and phenolic compounds

Water and wastewater purification by adsorption is one of the easiest and most economic processes used for organic and inorganic pollutants removal (Wang, Zhao, et al., 2018). Furthermore, coal ash-based entities have been widely used as adsorbents for toxic metals and phenolic compounds remediation. In this section, we describe some synthesized adsorbents using coal ash including coal fly ash and bottom as inorganic supports, preparation methods, and

characterization techniques employed to provide the successful functionalization of coal ash based-materials. The application of these adsorbents to remove heavy metals and phenolic compounds from wastewater is outlined in this section.

Wang, Chen, et al. (2022) developed inexpensive, recyclable and highly-effective uranium (U (VI)) adsorbent material *via* the calcination-freeze-drying technology (Figure S5). In this study, the authors showed that the elimination percentage of uranium U (VI) by fly ash aerogel in shape reached 94.5% at pH equal to 3.0 and a maximum removal capacity of uranium U (VI) was attained 110.73 mg·g<sup>-1</sup> at room temperature. Thus, the structural analysis including scanning electron microscopy (SEM), X-ray diffraction (XRD), Fourier-transform infrared spectroscopy (FTIR) and X-ray photoelectron spectroscopy (XPS) demonstrated that a successful transformation of fly ash and uranium U (VI) was successfully adsorbed on fly ash aerogel by complexation mechanism (Figure S6). The authors concluded that the effectiveness of the adsorption behavior of uranium U (VI) on fly ash based-material depends mainly on the grafted groups on the surface of the synthesized aerogel (SiO<sup>-</sup>, AlO<sup>-</sup>, and OH<sup>-</sup>).

Zhao et al. (2021) utilized the hydrothermal method to prepare modified coal fly ash by NaOH (NMFA). This one-step calcination greatly simplified the process of preparing the adsorbent with ratio equal to 5.0:5.0 at 200 °C and calcination time equal to 3.0h. The researchers applied SEM, XRD, FTIR, XPS and Brunauer-Emmett-Teller (BET) to confirm the synthesis of the adsorbent. Moreover, Zhao's group indicated that the modified coal fly ash has a rougher surface structure compared to the raw coal fly ash. The obtained adsorbent contains full of pore structure and larger with chemical binding energy after modification, indicating a change of the functional group into the coal fly ash. Zhao's group revealed that the specific surface area increased from 12.475 m<sup>2</sup>·g<sup>-1</sup> to 37.176 m<sup>2</sup>·g<sup>-1</sup> when the ratio of coal fly ash: NaOH increases from 5:3 to 5:5. This rise highlights the role of NaOH on the porosity modification of coal fly ash. The XRD spectra showed the molecular formula of 1.08Na<sub>2</sub>O·Al<sub>2</sub>O<sub>3</sub>·1.68SiO<sub>2</sub>·1.8H<sub>2</sub>O (zeolite material) confirming the raw fly ash transformation by NaOH solution. In this process, the authors applied the as-prepared adsorbent for Cd (II) removal at a time interval (1.0-180 min), pH solutions (2.0-7.0), temperatures (25, 35, 45, and 55 °C) and coexisting of the following cations (Mg<sup>2+</sup>, Na<sup>+</sup>, Ca<sup>2+</sup>, and K<sup>+</sup>). The obtained findings proved the successful removal of Cd (II) with a 91.2% of removal percentage and 91.2 mg·g<sup>-1</sup> of maximum adsorption capacity at pH equal to 4.0 (Zhao et al., 2021). It was observed that the presence of the coexisting cations resulted in the decrease of Cd (II) adsorption. Besides, the inhibition of cadmium Cd (II) removal in the presence of different cations was (Ca<sup>2+</sup> > Mg<sup>2+</sup> > Na<sup>+</sup> > K<sup>+</sup>).

Huda et al. (2021) synthesized dithizone-coal bottom ash to remove lead (Pb (II)) ion from aqueous solution. In this study, the authors applied FTIR, transmission electron microscopy (TEM), XRD, scanning electron microscopy-energy dispersive X-ray spectroscopy (SEM-EDX) and differential scanning calorimetry and thermogravimetric analysis (DSC and TGA) to confirm the successful immobilization of dithizone on bottom ash at 50 °C for 16h of contact time. They showed that the synthesized adsorbent has a good affinity toward Pb (II) with a maximum adsorption capacity equal to 31.25 mg·g<sup>-1</sup> and the adsorption is governed by hydrogen bond and electrostatic interactions (Huda et al., 2021).

In order to ameliorate the efficiency of raw fly ash in removing phenolic compounds, Oyehan's group studied mesoporous acid-treated fly ash coated cationic polydiallyldimethyl ammonium chloride (PDDA) for phenol removal (Oyehan et al., 2020). In their work, the authors used SEM-EDX, Raman spectroscopy, FTIR and TGA to confirm the successful film coating. In their work, the authors used SEM-EDX, Raman spectroscopy, FTIR and TGA to confirm the successful film coating (Figure 2). Oyehan et al. (2020) proved that the modification of raw fly ash with acid converted more sp<sup>3</sup> into sp<sup>2</sup> due to its oxidation in the presence of (COO<sup>-</sup>) and (OH). Regarding the effectiveness and affinity of the synthesized material for phenol removal, the researchers found that PDDA-FA obtained using ultrathin coating layer-by-layer method exhibited a high phenol removal (95%) at room temperature and pH equal to 7.0. Furthermore, the applied mechanism of phenol adsorption was physical, and the fly ash-based adsorbent was well reused

after phenol adsorption in aqueous phase. Then, the reported adsorbents were considered as eco-friendly using a green synthesis approach for new cleaner production showing higher adsorption capacities toward toxic pollutant by coal ash derivatization. Table S1 defines other reported coal ash based-adsorbents and demonstrates the increase of interest in these materials for toxic metals and phenolic compounds removal including the abovementioned adsorbents (Bada et al., 2013; Huda et al., 2021; Joseph et al., 2020; Min et al., 2021; Oyehan et al., 2020; Pan et al., 2013; Qi et al., 2019; Shah et al., 2017; Vu et al., 2020; Wang, Hao, et al., 2018; Wang, Chen, et al. 2022; Zhao et al., 2021).

### 3.2. Kinetic and equilibrium adsorption models

#### 3.2.1. Adsorption kinetics

The kinetics of the toxic metals and phenolic compounds by adsorption gives important information about the residue uptake rate and the reaction behavior between the adsorbent and each pollutant. Moreover, to study toxic metals and phenolic compounds adsorption on solid surface, it can be taken into account to depict the residue removal process. Toxic metals and phenolic compounds removal by coal ash derivatives was investigated, in the literature, by three kinetic models: the pseudo- first-order, the pseudo-second-order and the external-intraparticle diffusion

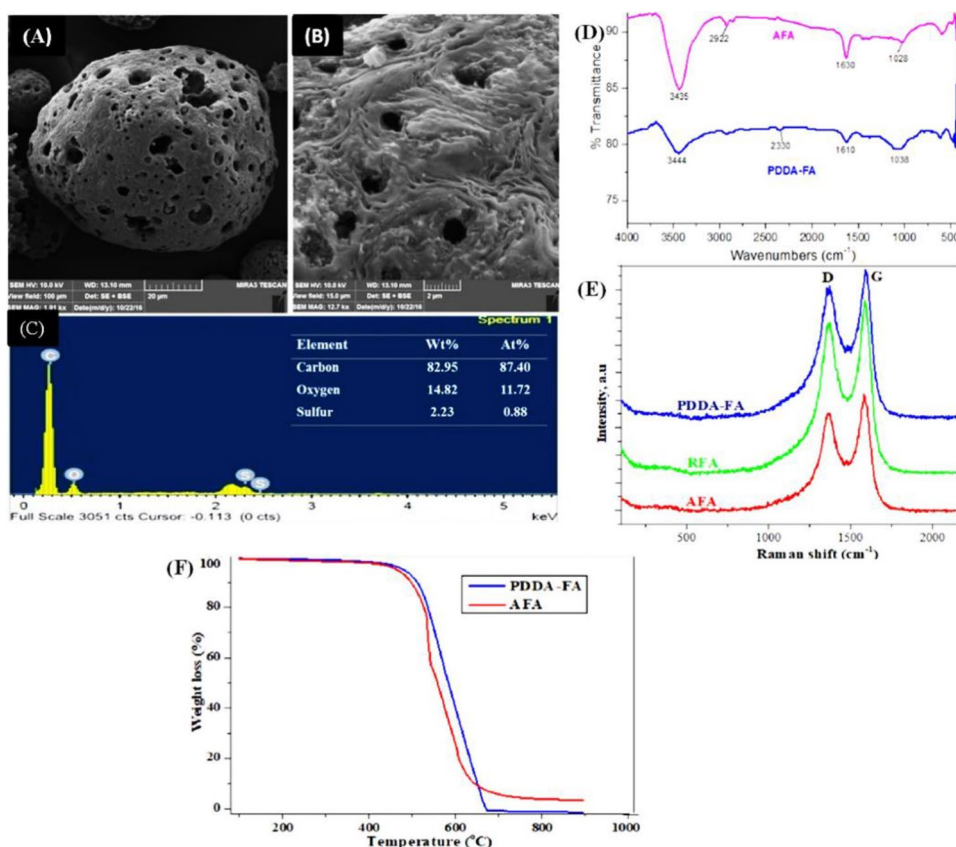


**Figure 2.** SEM micrographs of a single particle of PDDA-coated FA at magnification of (A) 1,910x (B) 12,700x. (C) EDX spectrum of PDDA-FA with weight and atomic percent of component elements in an embedded table, (D) IR spectra of AFA, and PDDA-FA (E) Raman spectra of RFA, AFA, and PDDA-FA; (F) TGA spectra of AFA and PDDA-FA. Reprinted with permission of Elsevier from Oyehan et al. (2020). SEM: Scanning electron microscopy, PDDA: Polydiallyldimethyl ammonium chloride, FA: Fly ash, EDX: Energy dispersive X-ray spectroscopy, PDDA-FA: Polydiallyldimethyl ammonium chloride coated fly ash, IR: Infrared spectra, AFA: Acid-treated fly ash, RFA: Raw fly ash, TGA: Thermogravimetric analysis.

kinetic models (An et al., 2016; Buema et al., 2021; Mofulatsi et al., 2022; Repo, 2011). Kinetic models are discussed in Supporting Information (Sec. S 3.2.1).

Several works reported the adsorption kinetics of toxic metals and phenolic compounds on coal ash-based materials. They also indicated that the adsorption generally followed the second-order kinetic model. Among them, An et al. (2016) investigated the sulfonated humic acid (SHA, phenolic compound) adsorption on the modified coal fly ash waste. An's group demonstrated that the SHA removal by the modified fly ash can be better fitted by the pseudo-second-order kinetic model. Thus, the adsorption mechanism seems to be controlled by the chemisorption process. In another work, Mofulatsi's coworkers examined coal fly ash coating by manganese oxide for Pb (II) adsorption (Mofulatsi et al., 2022). The authors concluded that the adsorption kinetics followed the non-linear Elovich kinetic model and provided a better fit compared to the pseudo-first-order and pseudo-second-order, which indicated a heterogeneous adsorption process by electrostatic interaction and ion exchange (Figure S7, Mofulatsi et al., 2022).

### 3.2.2. Isotherms modeling

The adsorption isotherms of toxic metals and phenolic compounds were evaluated, in the literature, by means of isotherm curves such as Langmuir, Freundlich, MLF, Temkin, Dubinin-Radushkevich models, and so on (Repo, 2011). The nonlinear and linear fitting forms of these representations give an idea about the relationship between the quantity of toxic metals and phenolic compounds adsorbed on coal ash-based materials ( $q_e$ , mg. g<sup>-1</sup>) and the residual mass of heavy metals and phenolic compounds after reaching the equilibrium process in solution ( $C_e$ , mg. L<sup>-1</sup>) under optimum conditions at a given temperature and specific pH (An et al., 2016; Buema et al., 2021; Repo, 2011; Wang et al., 2014). The different isotherm models are discussed further in Supporting Information (Sec. S 3.2.2). In addition to the study of the adsorption kinetics, isotherms and the effect of the different parameters for each pollutant removal (i.e. effect of contact time, adsorbent dose, temperature (thermodynamic studies), initial concentration, pH, among others.) which were intensively examined in previous research works (Dogar et al., 2020; Karanac et al., 2018; Tahari et al., 2021) to get an insight about the mechanism of pollutants adsorption. Furthermore, the reusability of the adsorbent materials is an important step that was dealt with in several scientific publications investigating the stability of the used adsorbents and their application in columns (continuous adsorption) and in real wastewater (industrial reject) treatment.

### 3.3. Advantages and disadvantages

The literature survey demonstrates that adsorption process is one of the effective and economic techniques utilized to remove toxic metals and phenolic compounds from real and synthetic wastewater. Compared to other processes (i.e. biological treatment, coagulation, and ion exchange oxidation), adsorption process has its own benefits and limitations (Patel, 2021; Yagub et al., 2014; Zhu et al., 2019). The benefits of various adsorbents-based on coal ash for toxic metals and phenolic compounds removal are as follows:

1. The method employs a simple column (fixed bed) in continuous adsorption and discontinuous adsorption experiments (batch systems) for toxic metals and phenolic compounds decontamination (An et al., 2016; Mofulatsi et al., 2022). Besides, adsorption is considered as the most economic approach widely used for these harmful pollutant removal.
2. As low-cost industrial wastes, fly ash and bottom ash contain aluminum oxides, iron oxides, melite and merwinite that are related to MgO and silica. The presence of these compounds in coal ash and bottom has many benefits such porosity, morphology, large surface area, suitable functionalization and consequently a good adsorption capacity toward phenolic compounds and toxic metals removal.

3. For example, the overflow of the adsorbents with the phenolic compounds or toxic metals can be solved by using magnetic coal fly ash or bottom ash that allows easily separating, washing and reusing the adsorbents. Thus, the adsorption process becomes highly-effective even at low concentration levels of phenolic compounds and toxic metals in contaminated water.
4. It has been found that the porosity of coal fly ash and bottom ash play a crucial role in the inorganic and organic entities insertion and, then, in coal ashes transformation. Therefore, phenolic compounds and toxic metals can be more adsorbed on coal ash-based materials due to the good interactions between the adsorbed molecules and the modified adsorbents.
5. Technologically, the adsorption process is simple and sustainable in term of toxic metals and phenolic compounds removal from wastewater. It works at suitable operating conditions and at a wide pH range, different temperatures, fast contact time, other cation and anion ions existing in solution, single and binary system of target pollutants (Patel, 2021).
6. Coal fly ash and bottom ash show high efficiency in toxic metals and phenolic compounds removal, simple and robust adsorbents, suitable for discontinuous/continuous adsorption process, and easy to maintain in different conditions.
7. Industrially, the feasibility of adsorption process is considered as one of the most important treatments in effluents removal including toxic metals and phenolic compounds (Zhu et al., 2019).

In the other hand, adsorption has certain disadvantages such as adsorbents are very costly in some cases, discharge of solid waste in water and soil (used adsorbents). Other disadvantages of adsorption process stated bellow:

1. The hard separation of the coal fly ash and bottom ash derivatives after their application in phenolic compounds and toxic metals removal is one of the major problems in the adsorption process.
2. In some cases, coal ash-based adsorbents become inactive and exhausted and their recuperation using the adequate desorbing agent represents a critical issue. Moreover, some desorbing agents are highly expensive. They create air pollution and acidic surface, block, and degrade the pores of adsorbents. Consequently, the hardness of coal ash-based adsorbents generation after their applications in wastewater remediation is still the main challenges for researchers and industries.
3. In addition, some coal fly ash and bottom ash derivatives cannot be applied in continuous adsorption (fixed bed) due to their agglomeration. Besides, adsorption shows some difficulty in terms of isotherm modeling and adsorption kinetics, which led, in some cases to the poor study of the adsorption mechanism of phenolic compounds and toxic metals removal.

## **4. Ceramic membranes for wastewater remediation**

### **4.1. Toxic metals and phenolic compounds separation**

In recent years, membrane separation process including microfiltration, ultrafiltration, nanofiltration and reverse osmosis has been developed as one of the most common eco-friendly and easy methods applied in water and wastewater treatment (Ge et al., 2015; Rani et al., 2021). As shown in Figure 3, ceramic membranes based on low-cost raw materials are prepared in different configurations, namely flat and tubular, using various fabrication methods, for example, powder pressing, paste casting, extrusion, tape casting, slip casting, phase inversion and freeze casting (Rani & Kumar, 2021). Membrane separations are widely employed in sewage treatment and wastewater containing toxic metals and phenolic compounds by conducting a lab-scale experiments (Hubadillah et al., 2019). On the one hand, the thermal treatment and sintering

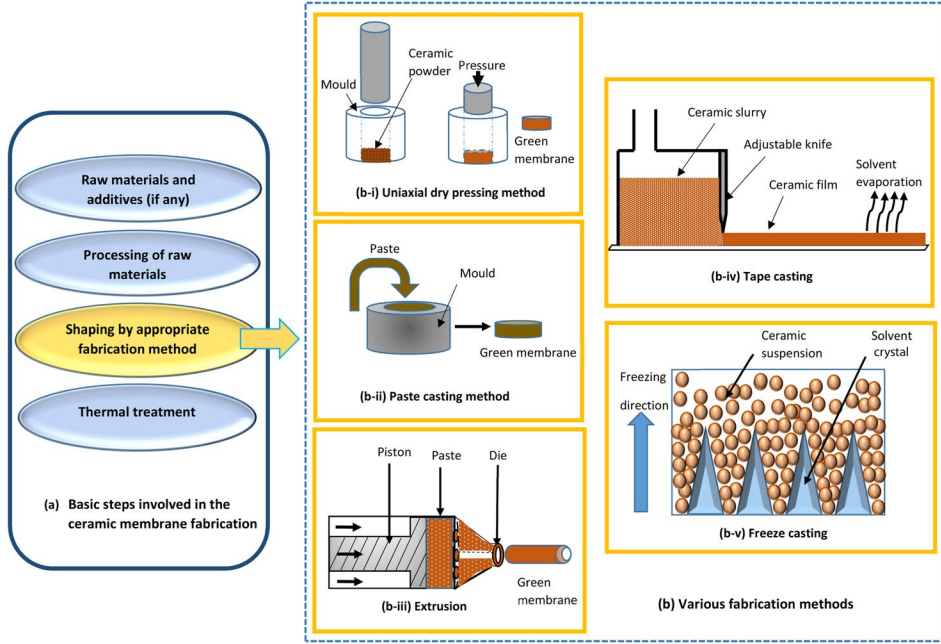


**Figure 3.** Fabrication methods to prepare ceramic supports. Reprinted with permission of Elsevier from Rani and Kumar (2021).

temperature are essential parameters in the synthesis of these ceramic membranes (Ge et al., 2015). On the other hand, the linear variation of the membrane permeate flux ( $J$ ) with the pressure difference ( $\Delta P$ ) is in agreement with the theoretical equation proposed by Kozeny–Carman given by the following equation (Equation (2)) usually applied to study the membranes properties (Fang et al., 2013; Li, Bai, et al., 2022).

$$J = \frac{\Delta P \theta^3}{K_0 K_t L \eta S_v^2 (1 - \theta)^2} \quad (2)$$

where ( $K_0$ ) and ( $K_t$ ) are the membrane constants, ( $\theta$ ) represents the porosity, ( $L$ ) is the membrane thickness and ( $S_v$ ) corresponds to the internal surface area of the solution. Other theoretical models employed to investigate membrane in wastewater treatment (i.e. hydrodynamic, concentration polarization, pore-blocking and resistance-in-series models, etc.) were also reported (Fang et al., 2013; Li, Bai, et al., 2022).

The pore-blocking model equations including complete pore blocking, standard pore blocking, intermediate pore blocking and cake filtration are formulated employing the following linearized equations of membrane permeation flux ( $J$ ) and time ( $t$ ) (Equations (3)–(6), (Fang et al., 2013)).

$$\ln(J^{-1}) = \ln(J_0^{-1}) + K_b t : \text{Complete pore blocking} \quad (3)$$

$$J^{-0.5} = J_0^{-0.5} + K_s t : \text{Standard pore blocking} \quad (4)$$

$$J^{-1} = J_0^{-1} + K_i t : \text{Intermediate pore blocking} \quad (5)$$

$$J^{-2} = J_0^{-2} + K_c t : \text{Cake filtration} \quad (6)$$

The resistance-in-series (RIS) model widely applied to describe the membrane resistance is presented below (Equation (7)):

$$J = \frac{\Delta P_m}{\mu(R_t)} = \frac{\Delta P_m}{\mu(R_m + R_{re} + R_{irr})} \quad (7)$$

where ( $J$ ) represents the permeate flux ( $\text{m}\cdot\text{s}^{-1}$ ), ( $\Delta P_m$ ) denotes the transmembrane pressure (Pa), ( $\mu$ ) is the dynamic viscosity ( $\text{Pa}\cdot\text{s}^{-1}$ ), ( $R_t$ ) corresponds to the total membrane resistance ( $\text{m}^{-1}$ ), ( $R_m$ ) designates the cleaned membrane resistance ( $\text{m}^{-1}$ ), ( $R_{ir}$ ) is the irreversible resistance (owing to adsorption, internal pore blocking, etc.) ( $\text{m}^{-1}$ ), and ( $R_{re}$ ) refers to the reversible resistance (Fang et al., 2013).

Moreover, introducing a membrane entity or transforming coal ash on porous membranes offers an almost complete separation of residues and several benefits in wastewater remediation due to the porosity and high accessibility of raw coal ash and its chemical and thermal stability even at high temperature. Ceramic membranes based on coal ash have been intensively examined by the research community. In this section, some selected coal ash loaded membranes or the transformation of these materials into porous ceramic membranes to remove or minimize toxic metals and phenolic compounds from aqueous medium will be outlined.

Zhu et al. (2018) synthesized  $\text{Al}_2\text{O}_3$ -NaA zeolite composite hollow fiber membrane based on coal fly ash using the hydrothermal method. They applied XRD and SEM analysis to confirm the synthesis of membrane. The size and porosity of the membrane were calculated by a laser particle size and a pore size distribution analyzer, respectively. The as synthesized membrane had a pore size of 0.41  $\mu\text{m}$ , a thickness of  $\sim 6.0$  mm and contained a considerable amount of (NaA) crystals. The authors applied the as-synthesized membrane to pre-concentrate Pb (II) under the following conditions (50  $\text{mg}\cdot\text{L}^{-1}$  of Pb (II), 0.1 MPa trans-membrane pressure, temperature of 25 °C and 12 h of filtration time. The experimental results confirmed the good efficiency of the porous membrane in removing of Pb (II) (higher than 99%) and the main mechanism of Pb (II) was explained based on the adsorption of the metal on the membrane surface. Zhu's coworkers proved that coal fly ash can be an effective method by recycling this material to manage waste rich with heavy metals like Pb (II).

In another study, Zhang, Yan, et al. (2021) utilized fly ash to remove simultaneously Cu (II), Cd (II) and Cr (VI) using porous ceramic fly ash as support loaded by ( $\text{TiO}_2$ ) nanofiber membrane. In this process, the authors employed the hydrothermal method relying on fly ash, industrial rutile and graphite. In this green preparation method, TNM-PFACS porous material was characterized by TEM, SEM-EDX and XRD (Figure 4) to get insight about the morphology of the synthesized material. The authors concluded that TNM-PFACS are formed by two layers including macro-porous layer (porous fly ash ceramic support, PFACS having a pore diameter of 2.0–8.0  $\mu\text{m}$  and a mesoporous layer ( $\text{TiO}_2$  nanofiber membrane, TNM) formed by  $\text{TiO}_2$  nanofibers with a diameter of 10–30 nm with a thickness equal to 10  $\mu\text{m}$ . The main phases of the synthesized material are composed of cristobalite ( $\text{SiO}_2$ , tetragonal system), mullite ( $3\text{Al}_2\text{O}_3\cdot 2\text{SiO}_2$ , orthorhombic) and anorthite system ( $8\text{CaO}\cdot 8\text{Al}_2\text{O}_3\cdot 16\text{SiO}_2$ ). The obtained results confirmed the effective loading of  $\text{TiO}_2$  on fly ash inorganic material (Zhang, Yan, et al., 2021). In fact, the examined material was used in membrane process of two heavy metals (Cu (II) and Cd (II)) separation and Cr (VI) reduction in the presence of rhodamine B under the following conditions (contact time of 240 min using 100  $\text{mg}\cdot\text{L}^{-1}$  of each pollutant and water flux equal to 223  $\text{L}\cdot\text{m}^{-1}\cdot\text{h}^{-1}\cdot\text{bar}^{-1}$ ). The experimental findings revealed that the efficiency removal percentage of 90.15% and the maximum adsorption capacity (9.56  $\text{mg}\cdot\text{g}^{-1}$ ) of Cu (II) were reached while the removal of Cd (II) was inhibited, rhodamine B in solution promoted greatly toxic Cr (VI) reduced to Cr (III) and the highest removal percentage of Cr (VI) attained 97.09%. In this study, the authors concluded that removal of the studied metals was physical adsorption driven by electrostatic forces. In accordance with these results, the synthesized materials reused after many cycles of adsorption/desorption showed a good affinity toward different pollutants due to the availability of good surface area in TNM-PFACS and electrostatic interactions between the membrane and heavy metals (Zhang, Yan, et al., 2021). In another study, Gupta et al. (2019) investigated the efficiency of dead-end filtration setup process in removing phenol in aqueous phase utilizing choline chloride and cellulose acetate to synthesize a porous membrane based on fly ash. Besides, the authors employed raw fly ash as inorganic support and a simple coating method to fabricate the cross-linked membrane.

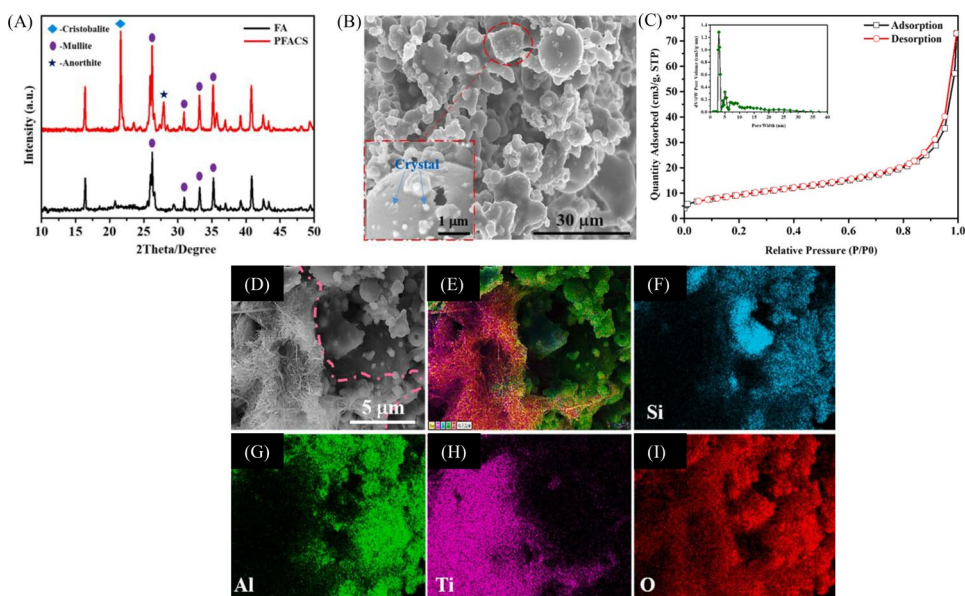


**Figure 4.** XRD patterns (A) and microstructure (B) of PFACS. Inset: mullite crystals on the surface of FA. SEM images and elemental analyses of the TNM-PFACS, adsorption-desorption isotherms; inset: the pore size distribution of TNM (C) and SEM images and elemental analyses of the TNM-PFACS (D-I). Reprinted with permission of Elsevier from Zhang et al. (2021). PFACS: Porous fly ash ceramic support, TNM: TiO<sub>2</sub> nanofiber membrane, TNM- PFACS: TiO<sub>2</sub> nanofiber membrane-porous fly ash ceramic support.

The as-obtained membrane-based on fly ash was well characterized by the contact angle, SEM, FTIR, swelling test and its permeability to transform raw ash into porous membrane. The experimental results showed that porous membrane needed a 207 kPa as good pressure to reach the high permeation flux (1.54 L·m<sup>-2</sup>·h<sup>-1</sup>). During this process, the fly ash-based membrane was applied for filtration removal of phenol ( $C_0 = 100 \text{ mg}\cdot\text{L}^{-1}$ , pH = 10). The authors demonstrated that, during the membrane filtration, its rejection rate toward phenol remained superior to 92% and the permeation rate was high (Gupta et al., 2019). According to the existing literature, coal ash is an effective support loaded or transformed into ceramic membranes. It shows a high affinity toward the removal of several pollutants from aqueous phase. Other derivatives of coal ash-based membranes including the above-mentioned membranes were applied for wastewater containing toxic metals and phenolic compounds remediation purposes (Supporting Information Table S2) (Gupta et al., 2019; Gupta & Anandkumar, 2019; He et al., 2020; Huang et al., 2020; Rawat & Bulasara, 2018; Yusof et al., 2020; Zhang, Yan, et al., 2021; Zhu et al., 2018).

#### 4.2. Advantages and limitations of ceramic membranes

The processes that use membranes to separate hazardous effluents offer exciting applications for toxic metals and phenolic compound treatment in degraded water and wastewater. Furthermore, the treatment of wastewater by membrane separation is one of the rare applied to treat solutions rich with toxic metals and phenolic compounds. However, membrane filtration process has some strengths and weaknesses (Belfort, 2019; Crini & Lichtfouse, 2019; Goswami & Pugazhenth, 2020; Rosman et al., 2018). Some of them are stated below:

- i. The advantages of membrane filtration for toxic metals and phenolic compounds separation are due to its rapid implementation with low space requirement. This method

- allows also removing these residues from wastewater without using harsh or expensive chemicals.
- ii. Membrane is a continuous separation process under easy conditions; remove all types of pollutants including toxic metals and phenolic compounds, high performance and simple operation. Its specific pore size makes it effective for a “first pass” filtration; separation can be carried out under any conditions, long term stability of membrane and at high temperature. It does not depend on pH, ionic strength, membranes properties can be adjusted and disinfection can be performed without chemicals.
  - iii. Ceramic membrane separation based on coal ash is the most environmentally sustainable process and often utilized as the most efficient technique in removing toxic metals and phenolic compounds from water phase.
  - iv. The major limitation of membrane filtration process for toxic metals and phenolic compounds separation is its limited lifetime and high cost before it happens fouling of the membrane and the industrial application of membrane process demand further requirement.
  - v. Membrane separation also results in concentration polarization membrane fouling, poor selectivity in some cases of toxic metals and phenolic compounds separation, limited sample volume, blocking problems, low permeability and high cost in some stage, hardness of membrane generation and its maintenance after uses.

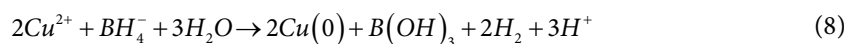
## 5. Coal ash-based photocatalysts

### 5.1. Photodegradation of toxic metals and phenolic compounds

Recently, extensive research work has been performed on the coal ash as inorganic support in the advanced oxidation processes (AOP<sub>s</sub>). Coal ashes including coal fly ash and bottom ash have been widely applied in wastewater remediation (Chuaicham, Inoue, Balakumar, Tian, Ohtani, et al., 2022; Chuaicham, Inoue, Balakumar, Tian, & Sasaki, 2022; Li et al., 2021; Nadeem et al., 2022; Özcan et al., 2021; Zhang, Yuan, et al., 2022). The physicochemical and mineralogical characters of coal ashes make them one of the low-cost and sustainable materials employed to elaborate novel photocatalysts. On the one hand, the transformation of coal ashes by hydrothermal, microwave irradiation and hydrothermal-chemical methods into the zeolite materials is a technique widely used in photocatalysis that utilizes the zeolite obtained from coal ash as inorganic support (Alberti et al., 2019; Wang, Jin, et al., 2022; Yang et al., 2016; Yang et al. 2017). On the other hand, zeolite materials developed from coal ash and applied for photocatalysts synthesis have been intensively used in wastewater purification technology. Inorganic entities, such as metal oxides in coal ash surfaces, have been also employed in photocatalysis where these materials are used as inorganic supports for wastewater remediation, and novel synthetic methods for coal ash functionalization have been developed. In this section, various porous materials derived from coal ash will be discussed for the degradation of phenolic compounds and photocatalytic reduction of toxic metals in wastewater.

In their recent work, Fu et al. (2018) have reported the synthesis of photoactive mineral ash from biomass by pyrolysis method. The structural analysis of mineral ash using elemental analysis, X-ray fluorescence spectroscopy XRF, dynamic light scattering (DLS) and XRD suggested the existence of potassium chloride, amorphous silica and minor potassium sulfate content with an average particle size equal to  $360 \pm 20$  nm. By way of electron paramagnetic resonance spectroscopy (EPR), the authors indicated that the sunlight irradiation of the obtained mineral ash can produce ( $\bullet\text{O}_2^-$ ) and ( $\bullet\text{OH}$ ) quantified by the generated 2,3-bis(2-methoxy-4-nitro-5-sulfophenyl)-2H tetrazolium-5-carboxanilide (XTT) formazan using XTT as the probe of  $\bullet\text{O}_2^-$ , and the formation of 2-hydroxyterephthalic acid (HTPA) using terephthalic acid (TPA) as the probe of  $\bullet\text{OH}$ , respectively (Fu et al., 2018). In this semi-green preparation method, the obtained mineral ash applied for Cr (VI) reduction under sunlight irradiation utilizing a cylindrical

polytetrafluoroethylene vessel positioned in a water-circulating jacket (Figure S8) and phenolic compounds as electron donors in solution created Cr (VI)/phenolic compounds/photocatalyst ternary systems. The authors concluded that the silicon and silicon carbide immobilized in the catalyst surface are creditable for the photo-reduction of Cr (VI) to Cr (II). As shown in Figure S9, the provided results confirmed the mineral ash efficiency in reducing Cr (VI) to Cr (II) (80%) through Cr(VI)/4-chlorophenol/dissolved fly ash ternary systems under the following conditions: 0.26 mM Cr (VI), electron donors (0.3 mM 4-chlorophenol) and 200 mg·L<sup>-1</sup> of catalyst (dissolved mineral ash) at 20 °C (Fu et al., 2018). Regarding the photodegradation of phenolic compounds, Park et al. (2020) have developed an easy and inexpensive photocatalyst based on (Cu) loading on fly ash surface to treat wastewater effectively. They have argued that this hybrid material was sustainable, eco-friendly and recyclable photocatalyst. The authors have also proven that Cu (0) nanoparticles were fully impregnated on the surface of washed fly ash according to the following equation (Equation (8)).



In this process, Park's et al. applied high resolution field emission scanning electron microscope-energy-dispersive X-ray spectroscopy HR-FESEM-EDS, XRD and XPS to get insight about the physicochemical characteristics of the synthesized catalyst (Cu/water washed coal fly ash, Cu/WFA). Through the applied analysis techniques, the authors showed that the Cu (0) impregnation did not considerably change the morphology of the WFA. Furthermore, the XRD analysis indicated that the important increase in the two peaks of Cu/WFA after 2.0 h of contact time attributed to Cu (111) and Cu (200), which reflected the presence of (Cu) on the WFA surface (Park et al., 2020). In addition, the XPS analysis revealed that the existence of two peaks at 932.4 and 933.9 eV, showing Cu (0) (60.6%) higher than CuO (39.4%), confirmed the Cu (0) nanoparticles loading on WFA surface (Figure S10). The study proved that the total degradation of p-nitrophenol (p-NP) exhibited by the as-synthesized catalyst was approximately 100% with 97% of p-aminophenol (p-AP) production is generally higher than that provided by various catalysts used in other works under suitable conditions ([catalyst]=0.40 g. L<sup>-1</sup>, [p-NP]=0.1 mM and [NaBH<sub>4</sub>]=50 mM). Moreover, the authors demonstrated that the high amount of Fe (II) produced by the presence of NaBH<sub>4</sub> may led to the reduction of Cu (II) to three intermediates (Cu (0), Cu (0)/Fe (II) and Cu (0)/Fe (III)), which are responsible for p-nitrophenol degradation by hydride transfer (Figure 5). This finding proves the potential of Cu/WFA as a low cost catalyst for phenolic compound photodegradation (Park et al., 2020). Other derivatives of coal ash-based catalysts, including the abovementioned materials for toxic metals and phenolic

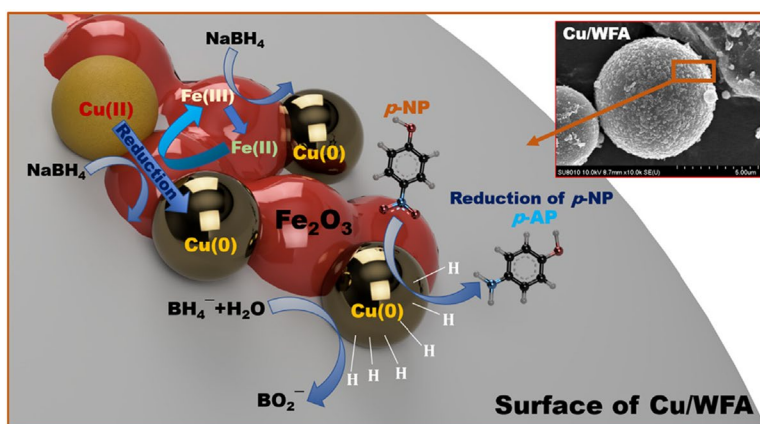


**Figure 5.** Reaction mechanism of Cu/WFA for reduction of p-NP to p-AP in the presence of NaBH<sub>4</sub>. Reprinted with permission of Elsevier from Park et al. (2020). WFA: Water washed coal fly ash, p-NP: p-Nitrophenol, p-AP: p-Aminophenol.

compounds photo-reduction and degradation respectively, were applied in wastewater treatment (Supporting Information Table S3) (Cao et al., 2021; Fu et al., 2018; Kim & Bae, 2018; Malakootian et al., 2016; Park & Bae, 2019; Subbulekshmi & Subramanian, 2017; Xu et al., 2019).

## 5.2. Benefits and limitations of photocatalysis

Photocatalysis technology using semiconductor materials has received much attention in the last decades. In this advanced technology, semiconductor materials adsorb light energy larger their band gap to generate excited electron ( $e^-$ ) and a positive hole ( $h^+$ ). Then, the oxygen molecules, present in the gas bubbles in the solution, are adsorbed on the catalyst surface to produce different oxygen species ( $^1O_2$ ,  $\cdot O_2^-$ ,  $H_2O_2$ , and  $\cdot OH$ ) (Equations (9)–(12)). The presence of these active species in liquid solution with visible light or solar irradiation can initiate the photoreduction of toxic metals and the phenolic compound photodegradation in contaminated water (Constantino et al., 2022; Wassel et al., 2020).



Due to its outstanding performance to degrade and reduce a large number of organic and inorganic residues under solar irradiation, this technology has been applied in industries of wastewater remediation (Constantino et al., 2022; Dell'Edera et al., 2021; Wassel et al., 2020; Su et al., 2019). Its advantages are mentioned below:

- The oxidation of large numbers of hazardous pollutants such as toxic metals and phenolic compounds and their degradation, which led to an effective environmental protection.
- Durability of the photocatalytic process and complete degradation of pollutants such as heavy metals and phenolic compounds.
- The application of photocatalysis technology does not lead to a secondary pollution.
- The high efficiency of photocatalysis process in wastewater remediation due to the coupling of this technique with other processes to achieve wastewater treatment goals and breaks the traditional concepts of photocatalysis application.

The uses of photocatalysis process in wastewater rich with toxic metals and phenolic compounds decontamination present some limitations:

- Difficult in catalysts separation after photocatalysis process from aqueous solution after particularly in the application of nanomaterials for toxic metals and phenolic compounds photodegradation.
- The lack of solar sensitivity and the rapid electron-hole ( $e^- / h^+$ ) recombination limits the performance of photocatalysts.
- Poor visible light activity of semiconductor materials and high gap energy and reusability of semiconductor materials are also a major limitation of photo catalytic process application in wastewater-containing toxic metals and phenolic compounds treatment.
- It is difficult to employ in the industrial applications of photocatalysis for toxic metals and phenolic compounds photodegradation due the high cost of some semiconductor materials.

## 6. Future perspectives

The demand for drinking water will increase considerably, in the coming years, all over the world. In this perspective, we show that the use of natural inorganic materials is a promising research area in water and wastewater remediation. Thus, the application of inorganic materials is much needed for toxic metals and phenolic compounds removal using adsorption, membrane filtration and photocatalysis processes. Actually, coal ashes disposal is being a global issue due to their production in large quantities. Thus, the “wastes -to- resource” like coal fly ash and bottom ash are inorganic materials characterized by their low-cost operations, eco-friendly, scalable, nontoxic and renewable characters. Taking in account their huge quantities, coal ash and their derivatives are also characterized by their ease of integration into the existing technologies of waste management. It is worthy to note that coal ashes are generally used in cementitious materials construction with a good thermal resistance, zeolites synthesis and can improve the quality of soil. Based on the chemical environment of Si and Al usually found in coal ash, these materials can act as a network former in the glass structure. Due to their advantages of abundant resources, these materials are ranked at the top of the most efficient and low-cost materials used for wastewater treatment due to their high porosity  $\sim 2.0\text{--}10\text{ nm}$ . Regardless of their application in wastewater treatment technologies, the current studied processes in this paper including adsorption, ceramic membrane and photocatalysis are the most applied and dominant industrial processes for waste management using several physical forms of coal ash. It is well known that these materials can be obtained from a variety of processes, such as coal combustion, that can be used in the future to remove toxic metals and phenolic compounds from wastewater.

1. There is a need to recycle coal ashes (coal fly ash and bottom ash) that will gain more intention in the future and will be considered as a new research area to achieve wastewater treatment purposes, especially for toxic metals and phenolic compounds remediation as assumed by many scientists and researchers.
2. It is worthy to note that the surface modification of pure coal ashes by introducing various organic and inorganic entities allows reducing toxic metals and phenolic compounds degradation may be intensively used in future application to remove toxic metals and phenolic compounds from wastewater.
3. The application of coal ashes adsorbents and ceramic membranes to treat toxic metals and phenolic compounds effluents should be further studied.
4. Various reported research works described the efficiency of coal ash-based materials in removing toxic metals and phenolic compounds in a single solution and in a binary or multi-pollutant system. Furthermore, it is obvious that coal ashes are promising materials in environmental remediation especially for wastewater treatment as good future perspectives in the uses of these naturel materials.
5. Recently, few research works have examined the role of coal ashes in the photocatalytic reduction of toxic metals. Therefore, the composition and characteristics of these low-cost materials should be further studied and their application in wastewater rich with toxic metals and phenolic compounds remediation has to be intensified.
6. In the future, other methods have to be developed to transform coal fly ash and bottom ash into sustainable and green materials to increase their efficiency to treat other emerging contaminants in wastewater such pharmaceutical products, industrial and household products, pesticides and micro-plastics. Moreover, soil decontamination and gases capture are crucial issues that should be dealt with urgently.

## 7. Conclusion

This review summarizes the purification of wastewater-containing toxic metals and phenolic compounds with coal ash as one of the most innovative low-cost raw materials. Exploring novel

synthetic methods (hydrothermal, microwave irradiation and alkaline fusion, etc.) and combining them with other techniques allow transforming raw coal ashes into other derivatives widely applied in wastewater treatment. The implementation of coal ash-based materials in this process requires also the introduction of appropriate new grafting groups like organic and inorganic entities. In fact, coal ash and their derivatives form various compounds are made up of effective adsorbents, membranes, and photocatalysts used to remove heavy metals and phenolic compounds. Coal ash-based materials show a high affinity toward these pollutants and are efficiently used to remove these hazardous effluents. Each process exhibits major benefits and limitations. Furthermore, these physiochemical properties were well confirmed by several techniques of analysis (i.e. FTIR, XRD, TEM, HR-TEM, SEM, XRF, XPS, etc.). The performance of coal ashes has been found to be the effect of the functional inorganic and organic groups immobilized on the surface of the coal fly ash and bottom ash as inorganic supports using several preparation methods. Mechanisms and parameters of toxic metals and phenolic compounds removal from contaminated water by each process were described and factors affecting the studied processes were also outlined. Taking in account the benefits and limitations of adsorption, membrane filtration and photocatalysis processes to remove toxic metals and phenolic compounds from wastewater, coal ashes including fly ash and bottom ash present a new trend in wastewater treatment technologies.

## Acknowledgements

The authors wish to acknowledge the School of Environmental Science and Engineering, Shaanxi University of Science and Technology for the financial support of this work.

## Disclosure statement

The authors declare that they have no known competing financial interests or personal relationships that could appeared to influence the work reported in this review paper.

## ORCID

Eric Lichtfouse  <http://orcid.org/0000-0002-8535-8073>

## References

- Abidin, Z., Prajaputra, V., Budiarti, S., Suryaningtyas, D. T., Matsue, N., & Sakakibar, M. (2021). Effect of alkaline concentrations on the synthesis of volcanic soil-based zeolite for methylene blue removal by fenton-like oxidation process. *Revista de Chimie*, 71(12), 47–55.
- Ajala, O. J., Khadir, A., Ighalo, J. O., & Umenweke, G. C. (2022). *Cellulose-based nano-biosorbents in water purification, nano-biosorbents for decontamination of water, air, and soil pollution*, 395–415. Elsevier.
- Akinterinwa, A., Usaku, R., Atiku, J. U., & Adamu, M. (2022). Focus on the removal of lead and cadmium ions from aqueous solutions using starch derivatives: A review. *Carbohydrate Polymers*, 290, 119463.
- Alawi, M., Torrijos, T. V., & Walsh, F. (2022). Plasmid-mediated antimicrobial resistance in drinking water. *Environmental Advances*, 8, 100191.
- Alberti, S., Caratto, V., Peddis, D., Belviso, C., & Ferretti, M. (2019). Synthesis and characterization of a new photocatalyst based on TiO<sub>2</sub> nanoparticles supported on a magnetic zeolite obtained from iron and steel industrial waste. *Journal of Alloys and Compounds*, 797, 820–825.
- Alterary, S. S., & Marei, N. H. (2021). Fly ash properties, characterization, and applications: A review. *Journal of King Saud University - Science*, 33(6), 101536.
- An, C., Yang, S., Huang, G., Zhao, S., Zhang, P., & Yao, Y. (2016). Removal of sulfonated humic acid from aqueous phase by modified coal fly ash waste: Equilibrium and kinetic adsorption studies. *Fuel*, 165, 264–271.
- Ayub, M. A., Ur Rehman, M. Z., Umar, W., Adnan, M., Farooqi, Z. U. R., Naveed, M., Aslam, M. Z., & Ahmad, H. R. (2021). Physiological mechanisms and adaptation strategies of plants under heavy metal micronutrient deficiency/toxicity conditions. *Frontiers in Plant-Soil Interaction*. Elsevier. 413–458.

- Bada, S., Potgieter, J., & Afolabi, A. (2013). Kinetics studies of adsorption and desorption of South African fly ash for some phenolic compounds. *Particulate Science and Technology*, 31(1), 1–9.
- Belfort, G. (2019). Membrane filtration with liquids: A global approach with prior successes, new developments and unresolved challenges. *Angewandte Chemie*, 131(7), 1908–1918.
- Bi, R., Yin, D., Lei, B., Chen, F., Zhang, R., & Li, W. (2022). Mercaptocarboxylic acid intercalated MgAl layered double hydroxide adsorbents for removal of heavy metal ions and recycling of spent adsorbents for photocatalytic degradation of organic dyes. *Separation and Purification Technology*, 289, 120741.
- Bing, H., Liu, Y., Huang, J., Tian, X., Zhu, H., & Wu, Y. (2022). Dam construction attenuates trace metal contamination in water through increased sedimentation in the Three Gorges Reservoir. *Water Research*, 217, 118419.
- Buema, G., Lupu, N., Chiriac, H., Ciobanu, G., Bucur, R.-D., Bucur, D., Favier, L., & Harja, M. (2021). Performance assessment of five adsorbents based on fly ash for removal of cadmium ions. *Journal of Molecular Liquids*, 333, 115932.
- Cao, J., Cui, Z., Wang, T., Zou, Q., Zeng, Q., Luo, S., Liu, Y., & Liu, B. (2021). Reductive removal of Cr (VI) by citric acid promoted by ceramsite particles: Kinetics, influential factors, and mechanisms. *Materials Today Communications*, 28, 102716.
- Cheng, Z., Yang, J., Li, L., Chen, Y., & Wang, X. (2022). Flocculation inspired combination of layered double hydroxides and fulvic acid to form a novel composite adsorbent for the simultaneous adsorption of anionic dye and heavy metals. *Journal of Colloid and Interface Science*, 618, 386–398.
- Cho, Y. K., Jung, S. H., & Choi, Y. C. (2019). Effects of chemical composition of fly ash on compressive strength of fly ash cement mortar. *Construction and Building Materials*, 204, 255–264.
- Chuaicham, C., Inoue, T., Balakumar, V., Tian, Q., Ohtani, B., & Sasaki, K. (2022). Visible light-driven ZnCr double layer oxide photocatalyst composites with fly ashes for the degradation of ciprofloxacin. *Journal of Environmental Chemical Engineering*, 10(1), 106970.
- Chuaicham, C., Inoue, T., Balakumar, V., Tian, Q., & Sasaki, K. (2022). Fabrication of visible-light-active ZnCr mixed metal oxide/fly ash for photocatalytic activity toward pharmaceutical waste ciprofloxacin. *Journal of Industrial and Engineering Chemistry*, 108, 263–273.
- Constantino, D. S., Dias, M. M., Silva, A. M., Faria, J. L., & Silva, C. G. (2022). Intensification strategies for improving the performance of photocatalytic processes: A review. *Journal of Cleaner Production*, 340, 130800.
- Crini, G., & Lichtfouse, E. (2019). Advantages and disadvantages of techniques used for wastewater treatment. *Environmental Chemistry Letters*, 17(1), 145–155.
- Cui, Y., Bai, L., Li, C., He, Z., & Liu, X. (2022). Assessment of heavy metal contamination levels and health risks in environmental media in the northeast region. *Sustainable Cities and Society*, 80, 103796.
- Dalanta, F., & Kusworo, T. D. (2022). Synergistic adsorption and photocatalytic properties of AC/TiO<sub>2</sub>/CeO<sub>2</sub> composite for phenol and ammonia–nitrogen compound degradations from petroleum refinery wastewater. *Chemical Engineering Journal*, 434, 134687.
- Dell'Edera, M., Porto, C. L., De Pasquale, I., Petronella, F., Curri, M. L., Agostiano, A., & Comparelli, R. (2021). Photocatalytic TiO<sub>2</sub>-based coatings for environmental applications. *Catalysis Today*, 380, 62–83.
- Dogar, S., Nayab, S., Farooq, M. Q., Said, A., Kamran, R., Duran, H., & Yameen, B. (2020). Utilization of biomass fly ash for improving quality of organic dye-contaminated water. *ACS Omega*, 5(26), 15850–15864.
- Du, Z., Gong, Z., Qi, W., Li, E., Shen, J., Li, J., & Zhao, H. (2022). Coagulation performance and floc characteristics of poly-ferric-titanium-silicate-chloride in coking wastewater treatment. *Colloids and Surfaces A: Physicochemical and Engineering Aspects*, 642, 128413.
- Fang, J., Qin, G., Wei, W., Zhao, X., & Jiang, L. (2013). Elaboration of new ceramic membrane from spherical fly ash for microfiltration of rigid particle suspension and oil-in-water emulsion. *Desalination*, 311, 113–126.
- Ferreira, S., Meunier, S., Heinrich, M., Cherni, J. A., Darga, A., & Quéval, L. (2022). A decision support tool to place drinking water sources in rural communities. *The Science of the Total Environment*, 833, 155069.
- Fu, H., Li, Z., Zhang, Y., Zhang, H., & Chen, H. (2022). Preparation, characterization and properties study of a superhydrophobic ceramic membrane based on fly ash. *Ceramics International*, 48(8), 11573–11587.
- Fu, H., Zhou, Z., Zheng, S., Xu, Z., Alvarez, P. J., Yin, D., Qu, X., & Zhu, D. (2018). Dissolved mineral ash generated by vegetation fire is photoactive under the solar spectrum. *Environmental Science & Technology*, 52(18), 10453–10461.
- Gangani, N., Joshi, V. C., Sharma, S., & Bhattacharya, A. (2022). Fluoride contamination in water: Remediation strategies through membranes. *Groundwater for Sustainable Development*, 17, 100751.
- Gao, K., & Iliuta, M. C. (2022). Trends and advances in the development of coal fly ash-based materials for application in hydrogen-rich gas production: A review. *Journal of Energy Chemistry*, 73, 485–512.
- Ge, Y., Yuan, Y., Wang, K., He, Y., & Cui, X. (2015). Preparation of geopolymer-based inorganic membrane for removing Ni<sup>2+</sup> from wastewater. *Journal of Hazardous Materials*, 299, 711–718.
- Giri, T. K., & Badwaik, H. (2022). Understanding the application of gum ghatti based biodegradable hydrogel for wastewater treatment. *Environmental Nanotechnology, Monitoring & Management*, 17, 100668.

- Glasner, B., Henríquez-Castillo, C., Alfaro, F., Trefault, N., Andrade, S., & De la Iglesia, R. (2021). Decoupling of biotic and abiotic patterns in a coastal area affected by chronic metal micronutrients disturbances. *Marine Pollution Bulletin*, 166, 111608.
- Goswami, K. P., & Pugazhenthii, G. (2020). Credibility of polymeric and ceramic membrane filtration in the removal of bacteria and virus from water: A review. *Journal of Environmental Management*, 268, 110583.
- Guo, L.-C., Lv, Z., Ma, W., Xiao, J., Lin, H., He, G., Li, X., Zeng, W., Hu, J., Zhou, Y., Li, M., Yu, S., Xu, Y., Zhang, J., Zhang, H., & Liu, T. (2022). Contribution of heavy metals in PM<sub>2.5</sub> to cardiovascular disease mortality risk, a case study in Guangzhou, China. *Chemosphere*, 297, 134102.
- Gupta, V., & Anandkumar, J. (2019). Synthesis of crosslinked PVA-ceramic composite membrane for phenol removal from aqueous solution. *Journal of the Serbian Chemical Society*, 84(2), 211–224.
- Gupta, V., Raja, C., & Anandkumar, J. (2019). Phenol removal by novel choline chloride blended cellulose acetate-fly ash composite membrane. *Periodica Polytechnica Chemical Engineering*, 64(1), 116–123.
- Hasan, M., Rahman, M., Al Ahmed, A., Islam, M. A., & Rahman, M. (2022). Heavy metal pollution and ecological risk assessment in the surface water from a marine protected area, Swatch of No Ground, north-western part of the Bay of Bengal. *Regional Studies in Marine Science*, 52, 102278.
- Hashim, H. S., Fen, Y. W., Omar, N. A. S., & Fauzi, N. I. M. (2021). Sensing methods for hazardous phenolic compounds based on graphene and conducting polymers-based materials. *Chemosensors*, 9(10), 291.
- Hashim, H. S., Fen, Y. W., Omar, N. A. S., Fauzi, N. I. M., & Daniyal, W. (2021). Recent advances of priority phenolic compounds detection using phenol oxidases-based electrochemical and optical sensors. *Measurement*, 184, 109855.
- He, P. Y., Zhang, Y. J., Chen, H., Han, Z. C., & Liu, L. C. (2020). Low-cost and facile synthesis of geopolymer-zeolite composite membrane for chromium (VI) separation from aqueous solution. *Journal of Hazardous Materials*, 392, 122359.
- Helmrich, S., Vlassopoulos, D., Alpers, C. N., & O'Day, P. A. (2022). Critical review of mercury methylation and methylmercury demethylation rate constants in aquatic sediments for biogeochemical modeling. *Critical Reviews in Environmental Science and Technology*, 52(24), 4353–4378.
- Huang, L., Wu, B., Wu, Y., Yang, Z., Yuan, T., Alhassan, S. I., Yang, W., Wang, H., & Zhang, L. (2020). Porous and flexible membrane derived from ZIF-8-decorated hyphae for outstanding adsorption of Pb<sup>2+</sup> ion. *Journal of Colloid and Interface Science*, 565, 465–473.
- Hubadillah, S. K., Othman, M. H. D., Ismail, A., Rahman, M. A., & Jaafar, J. (2019). A low cost hydrophobic kaolin hollow fiber membrane (h-KHFM) for arsenic removal from aqueous solution via direct contact membrane distillation. *Separation and Purification Technology*, 214, 31–39.
- Huda, B. N., Wahyuni, E. T., & Mudasir, M. (2021). Eco-friendly immobilization of dithizone on coal bottom ash for the adsorption of lead (II) ion from water. *Results in Engineering*, 10, 100221.
- Iqbal, K., Jiang, W., Ma, R., & Deng, C. (2022). Synthesis of large-scale total water network with multiple water resources under seasonal flow rate constraints. *Journal of Cleaner Production*, 337, 130462.
- Jabbar, K. Q., Barzinjy, A. A., & Hamad, S. M. (2022). Iron oxide nanoparticles: Preparation methods, functions, adsorption and coagulation/flocculation in wastewater treatment. *Environmental Nanotechnology, Monitoring & Management*, 17, 100661.
- Jain, S., & Tembhurkar, A. R. (2022). Sustainable amelioration of fly ash dumps linking bio-energy plantation, bioremediation and amendments: A review. *Journal of Environmental Management*, 314, 115124.
- Jayaranjan, M. L. D., Van Hullebusch, E. D., & Annachhatre, A. P. (2014). Reuse options for coal fired power plant bottom ash and fly ash. *Reviews in Environmental Science and Bio/Technology*, 13(4), 467–486.
- Jin, Y., Feng, W., Zheng, D., Dong, Z., & Cui, H. (2020). Structure refinement of fly ash in connection with its reactivity in geopolymerization. *Waste Management (New York, N.Y.)*, 118, 350–359.
- Joseph, I. V., Tosheva, L., & Doyle, A. M. (2020). Simultaneous removal of Cd (II), Co (II), Cu (II), Pb (II), and Zn (II) ions from aqueous solutions via adsorption on FAU-type zeolites prepared from coal fly ash. *Journal of Environmental Chemical Engineering*, 8(4), 103895.
- Joshi, N. C., & Gururani, P. (2022). Advances of graphene oxide based nanocomposite materials in the treatment of wastewater containing heavy metal ions and dyes. *Current Research in Green and Sustainable Chemistry*, 5, 100306.
- Ju, T., Han, S., Meng, Y., & Jiang, J. (2021). High-end reclamation of coal fly ash focusing on elemental extraction and synthesis of porous materials. *ACS Sustainable Chemistry & Engineering*, 9(20), 6894–6911.
- Karanac, M., Đolić, M., Veljović, Đ., Rajaković-Ognjanović, V., Veličković, Z., Pavićević, V., & Marinković, A. (2018). The removal of Zn<sup>2+</sup>, Pb<sup>2+</sup>, and As (V) ions by lime activated fly ash and valorization of the exhausted adsorbent. *Waste Management (New York, N.Y.)*, 78, 366–378.
- Keshvardoostchokami, M., Majidi, M., Zamani, A., & Liu, B. (2021). A review on the use of chitosan and chitosan derivatives as the bio-adsorbents for the water treatment: Removal of nitrogen-containing pollutants. *Carbohydrate Polymers*, 273, 118625.
- Kim, M., & Bae, S. (2018). Immobilization and characterization of Fe (0) catalyst on NaOH-treated coal fly ash for catalytic reduction of p-nitrophenol. *Chemosphere*, 212, 1020–1029.

- Korashy, H. M., Attafi, I. M., Famulski, K. S., Bakheet, S. A., Hafez, M. M., Alsaad, A. M., & Al-Ghadeer, A. R. M. (2017). Gene expression profiling to identify the toxicities and potentially relevant human disease outcomes associated with environmental heavy metal exposure. *Environmental Pollution (Barking, Essex : 1987)*, 221, 64–74.
- Labidi, A., Salaberria, A. M., Fernandes, S. C., Labidi, J., & Abderrabba, M. (2020). Microwave assisted synthesis of poly (N-vinylimidazole) grafted chitosan as an effective adsorbent for mercury (II) removal from aqueous solution: Equilibrium, kinetic, thermodynamics and regeneration studies. *Journal of Dispersion Science and Technology*, 41(6), 828–840.
- Lei, K., Pan, H.-Y., Zhu, Y., Chen, W., & Lin, C.-Y. (2021). Pollution characteristics and mixture risk prediction of phenolic environmental estrogens in rivers of the Beijing-Tianjin-Hebei urban agglomeration, China. *The Science of the Total Environment*, 787, 147646.
- Li, X., Bai, C., Qiao, Y., Wang, X., Yang, K., & Colombo, P. (2022). Preparation, properties and applications of fly ash-based porous geopolymers: A review. *Journal of Cleaner Production*, 359, 132043.
- Li, X., Huang, G., Wang, S., Li, Y., Zhang, X., & Zhou, X. (2022). An interval two-stage fuzzy fractional programming model for planning water resources management in the coastal region—A case study of Shenzhen, China. *Environmental Pollution (Barking, Essex : 1987)*, 306, 119343.
- Li, Q.-G., Liu, G.-h., Qi, L., Wang, H.-C., Ye, Z.-F., & Zhao, Q.-L. (2022). Heavy metal-contained wastewater in China: Discharge, management and treatment. *The Science of the Total Environment*, 808, 152091.
- Li, G., Teng, Q., Sun, B., Yang, Z., Liu, S., & Zhu, X. (2021). Synthesis scaly Ag-TiO<sub>2</sub> loaded fly ash magnetic bead particles for treatment of xanthate wastewater. *Colloids and Surfaces A: Physicochemical and Engineering Aspects*, 624, 126795.
- Liu, Y., Wang, P., Gojenko, B., Yu, J., Wei, L., Luo, D., & Xiao, T. (2021). A review of water pollution arising from agriculture and mining activities in Central Asia: Facts, causes and effects. *Environmental Pollution (Barking, Essex : 1987)*, 291, 118209.
- Li, J., Yang, Z.-l., Ding, T., Song, Y.-J., Li, H.-C., Li, D.-q., Chen, S., & Xu, F. (2022). The role of surface functional groups of pectin and pectin-based materials on the adsorption of heavy metal ions and dyes. *Carbohydrate Polymers*, 276, 118789.
- Li, Z., Zhang, C., Liu, H., Zhang, C., Zhao, M., Gong, Q., & Fu, G. (2022). Developing stacking ensemble models for multivariate contamination detection in water distribution systems. *The Science of the Total Environment*, 828, 154284.
- Loi, J. X., Chua, A., S. M., Rabuni, M. F., Tan, C. K., Lai, S. H., Takemura, Y., & Syutsubo, K. (2022). Water quality assessment and pollution threat to safe water supply for three river basins in Malaysia. *The Science of the Total Environment*, 832, 155067.
- Luo, M., Zhang, Y., Li, H., Hu, W., Xiao, K., Yu, S., Zheng, C., & Wang, X. (2022). Pollution assessment and sources of dissolved heavy metals in coastal water of a highly urbanized coastal area: The role of groundwater discharge. *The Science of the Total Environment*, 807(Pt 3), 151070.
- Malakootian, M., Mesdaghinia, A., & Rezaei, S. (2016). The Photocatalytic Removal of Ortho Chlorophenol from Aqueous Solution Using Modified Fly Ash-Titanium Dioxide. *Journal of Water and Wastewater; Ab va Fazilab (in persian)* 27, 14–21. [http://www.wwjournals.ir/article\\_12203.html?lang=en](http://www.wwjournals.ir/article_12203.html?lang=en).
- Mangi, S. A., Ibrahim, M. H. W., Jamaluddin, N., Arshad, M. F., Memon, F. A., Jaya, R. P., & Shahidan, S. (2018). A review on potential use of coal bottom ash as a supplementary cementing material in sustainable concrete construction. *International Journal of Integrated Engineering*, 10(9), 127–135.
- Meesala, C. R., Verma, N. K., & Kumar, S. (2020). Critical review on fly-ash based geopolymer concrete. *Structural Concrete*, 21(3), 1013–1028.
- Min, X., Han, C., Yang, L., & Zhou, C. (2021). Enhancing As (V) and As (III) adsorption performance of low alumina fly ash with ferric citrate modification: Role of FeSiO<sub>3</sub> and monosodium citrate. *Journal of Environmental Management*, 287, 112302.
- Mo, Z., Tai, D., Zhang, H., & Shahab, A. (2022). A comprehensive review on the adsorption of heavy metals by zeolite imidazole framework (ZIF-8) based nanocomposite in water. *Chemical Engineering Journal*, 443, 136320.
- Mofulatsi, M., Prabakaran, E., Velepini, T., Green, E., & Pillay, K. (2022). Preparation of manganese oxide coated coal fly ash adsorbent for the removal of lead and reuse for latent fingerprint detection. *Microporous and Mesoporous Materials*, 329, 111480.
- Mukherjee, A. G., Wanjari, U. R., Renu, K., Vellingiri, B., & Gopalakrishnan, A. V. (2022). Heavy metal and metalloid-induced reproductive toxicity. *Environmental Toxicology and Pharmacology*, 92, 103859.
- Nadeem, N., Yaseen, M., Rehan, Z. A., Zahid, M., Shakoore, R. A., Jilani, A., Iqbal, J., Rasul, S., & Shahid, I. (2022). Coal fly ash supported CoFe<sub>2</sub>O<sub>4</sub> nanocomposites: Synergetic Fenton-like and photocatalytic degradation of methylene blue. *Environmental Research*, 206, 112280.
- Omar, A., Arken, A., Wali, A., Gao, Y., Aisa, H. A., & Yili, A. (2022). Effect of phenolic compound-protein covalent conjugation on the physicochemical, anti-inflammatory, and antioxidant activities of silk sericin. *Process Biochemistry*, 117, 101–109.
- Oyehan, T. A., Olabemiwo, F. A., Tawabini, B. S., & Saleh, T. A. (2020). The capacity of mesoporous fly ash grafted with ultrathin film of polydiallyldimethyl ammonium for enhanced removal of phenol from aqueous solutions. *Journal of Cleaner Production*, 263, 121280.

- Özcan, M., Birol, B., & Kaya, F. (2021). Investigation of photocatalytic properties of TiO<sub>2</sub> nanoparticle coating on fly ash and red mud based porous ceramic substrate. *Ceramics International*, 47(17), 24270–24280.
- Pan, J., Li, L., Hang, H., Ou, H., Zhang, L., Yan, Y., & Shi, W. (2013). Study on the nonylphenol removal from aqueous solution using magnetic molecularly imprinted polymers based on fly-ash-cenospheres. *Chemical Engineering Journal*, 223, 824–832. <https://www.sciencedirect.com/science/article/pii/S1385894713001654#1>.
- Park, J., & Bae, S. (2019). Highly efficient and magnetically recyclable Pd catalyst supported by iron-rich fly ash@ fly ash-derived SiO<sub>2</sub> for reduction of p-nitrophenol. *Journal of Hazardous Materials*, 371, 72–82.
- Park, J., Saratale, G. D., Cho, S.-K., & Bae, S. (2020). Synergistic effect of Cu loading on Fe sites of fly ash for enhanced catalytic reduction of nitrophenol. *The Science of the Total Environment*, 705, 134544.
- Patel, H. (2021). Review on solvent desorption study from exhausted adsorbent. *Journal of Saudi Chemical Society*, 25(8), 101302.
- Picetti, R., Deeney, M., Pastorino, S., Miller, M. R., Shah, A., Leon, D. A., Dangour, A. D., & Green, R. (2022). Nitrate and nitrite contamination in drinking water and cancer risk: A systematic review with meta-analysis. *Environmental Research*, 210, 112988.
- Picos-Corrales, L. A., Sarmiento-Sánchez, J. I., Ruelas-Leyva, J. P., Crini, G., Hermosillo-Ochoa, E., & Gutierrez-Montes, J. A. (2020). Environment-friendly approach toward the treatment of raw agricultural wastewater and river water via flocculation using chitosan and bean straw flour as bioflocculants. *ACS Omega*, 5(8), 3943–3951.
- Pu, M., Ailijiang, N., Mamat, A., Chang, J., Zhang, Q., Liu, Y., & Li, N. (2022). Occurrence of antibiotics in the different biological treatment processes, reclaimed wastewater treatment plants and effluent-irrigated soils. *Journal of Environmental Chemical Engineering*, 10(3), 107715.
- Qi, L., Teng, F., Deng, X., Zhang, Y., & Zhong, X. (2019). Experimental study on adsorption of Hg (II) with microwave-assisted alkali-modified fly ash. *Powder Technology*, 351, 153–158.
- Rajendran, S., Priya, A., Kumar, P. S., Hoang, T. K., Sekar, K., Chong, K. Y., Khoo, K. S., Ng, H. S., & Show, P. L. (2022). A critical and recent developments on adsorption technique for removal of heavy metals from wastewater-A review. *Chemosphere*, 303, 135146.
- Ramos, R. L., Moreira, V. R., Lebron, Y. A., Santos, L. V., & Amaral, M. C. (2022). Fouling in the membrane distillation treating superficial water with phenolic compounds. *Chemical Engineering Journal*, 437, 135325.
- Ramos, R. L., Moreira, V. R., Lebron, Y. A., Santos, A. V., Santos, L. V., & Amaral, M. C. (2021). Phenolic compounds seasonal occurrence and risk assessment in surface and treated waters in Minas Gerais—Brazil. *Environmental Pollution (Barking, Essex: 1987)*, 268(Pt A), 115782.
- Rani, S. L. S., & Kumar, R. V. (2021). Insights on applications of low-cost ceramic membranes in wastewater treatment: A mini-review. *Case Studies in Chemical and Environmental Engineering*, 4, 100149.
- Rani, N. H. A., Mohamad, N. F., Onn, M., Jalil, M. J., & Muda, N. (2021). Coal bottom ash as a potential adsorbent for CO<sub>2</sub> capture. In *IOP Conference Series: Materials Science and Engineering*. (Vol. 1176, No. 1, p. 12001). IOP Publishing.
- Rashidi, N. A., & Yusup, S. (2016). Overview on the potential of coal-based bottom ash as low-cost adsorbents. *ACS Sustainable Chemistry & Engineering*, 4(4), 1870–1884.
- Rawat, M., & Bulasara, V. K. (2018). Synthesis and characterization of low-cost ceramic membranes from fly ash and kaolin for humic acid separation. *Korean Journal of Chemical Engineering*, 35(3), 725–733.
- Ray, S. S., & Iroegbu, A. O. C. (2021). Nanocelluloses: Benign, sustainable, and ubiquitous biomaterials for water remediation. *ACS Omega*, 6(7), 4511–4526.
- Repo, E. (2011). EDTA-and DTPA-functionalized silica gel and chitosan adsorbents for the removal of heavy metals from aqueous solutions. Lappeenranta University of Technology Laboratory of Green Chemistry. <https://urn.fi/URN:ISBN:978-952-265-108-2>.
- Rosman, N., Salleh, W., Mohamed, M. A., Jaafar, J., Ismail, A., & Harun, Z. (2018). Hybrid membrane filtration-advanced oxidation processes for removal of pharmaceutical residue. *Journal of Colloid and Interface Science*, 532, 236–260.
- Said, K., A., M., Ismail, A., Zuhairun, A., Abdullah, M., Azali, M. A., & Abidin, M. N. Z. (2022). Magnetic induced asymmetric membrane: Effect of magnetic pattern to phenol removal by adsorption. *Materials Chemistry and Physics*, 278, 125692.
- Salam, M. A., Obaid, A. Y., El-Shishtawy, R. M., & Hussein, M. A. (2021). Preparation of novel magnetic chemically modified chitin nanocomposites and their application for environmental remediation of cadmium ions in model and real water samples. *Journal of Physics and Chemistry of Solids*, 148, 109748.
- Sanna, A., Thompson, S., Zajac, J., & Whitty, K. (2022). Evaluation of palm-oil fly ash derived lithium silicate for CO<sub>2</sub> sorption under simulated gasification conditions. *Journal of CO<sub>2</sub> Utilization*, 56, 101826.
- Shah, B. A., Pandya, D. D., & Shah, H. A. (2017). Impounding of ortho-chlorophenol by zeolitic materials adapted from bagasse fly ash: Four factor three level Box-Behnken design modelling and optimization. *Arabian Journal for Science and Engineering*, 42(1), 241–260.
- Sharma, C., Kashyap, D. K., Chaturvedi, A. K., Pappu, A., Chaurasia, J., Srivastava, A. K., & Gupta, M. K. (2022). Remarkable enhancement in dielectric constant and band gap shrinkage of hydrothermal grown fly ash waste derived zeolite nanoneedles. *Physica B: Condensed Matter*, 634, 413817.

- Sharma, N., Pap, Z., Kornélia, B., Gyulavari, T., Karacs, G., Nemeth, Z., Garg, S., & Hernadi, K. (2022). Effective removal of phenol by activated charcoal/BiOCl composite under UV light irradiation. *Journal of Molecular Structure*, 1254, 132344.
- Shen, B., Guo, Z., Huang, B., Zhang, G., Fei, P., & Hu, S. (2022). Preparation of hydrogels based on pectin with different esterification degrees and evaluation of their structure and adsorption properties. *International Journal of Biological Macromolecules*, 202, 397–406.
- Singh, N., Bhardwaj, & A., Shehnazdeep. (2020). Reviewing the role of coal bottom ash as an alternative of cement. *Construction and Building Materials*, 233, 117276.
- Some, S., Mondal, R., Mitra, D., Jain, D., Verma, D., & Das, S. (2021). Microbial pollution of water with special reference to coliform bacteria and their nexus with environment. *Energy Nexus*, 1, 100008.
- Soury, R., Jabli, M., Latif, S., Alenezi, K. M., El Oudi, M., Abdulaziz, F., Teka, S., El Moll, H., & Haque, A. (2022). Synthesis and characterization of a new meso-tetrakis (2, 4, 6-trimethylphenyl) porphyrinato) zinc (II) supported sodium alginate gel beads for improved adsorption of methylene blue dye. *International Journal of Biological Macromolecules*, 202, 161–176.
- Su, T., Qin, Z., Ji, H., & Wu, Z. (2019). An overview of photocatalysis facilitated by 2D heterojunctions. *Nanotechnology*, 30(50), 502002.
- Subbulekshmi, N., & Subramanian, E. (2017). Nano CuO immobilized fly ash zeolite Fenton-like catalyst for oxidative degradation of p-nitrophenol and p-nitroaniline. *Journal of Environmental Chemical Engineering*, 5(2), 1360–1371.
- Sun, S., Zhang, H., Luo, Y., Guo, C., Ma, X., Fan, J., Chen, J., & Geng, N. (2022). Occurrence, accumulation, and health risks of heavy metals in Chinese market baskets. *The Science of the Total Environment*, 829, 154597.
- Tahari, N., Nefzi, H., Labidi, A., Ayadi, S., Abderrabba, M., & Labidi, J. (2021). Removal of dyes and heavy metals with clays and diatomite, water pollution and remediation: Heavy metals, 539–569. Springer.
- Tan, H., Du, C., He, X., Li, M., Zhang, J., Zheng, Z., Su, Y., Yang, J., Deng, X., & Wang, Y. (2022). Enhancement of compressive strength of high-volume fly ash cement paste by wet grinded cement: Towards low carbon cementitious materials. *Construction and Building Materials*, 323, 126458.
- Taranu, B.-O., Vlazan, P., Svera, P., Poienar, M., & Sfirloaga, P. (2022). New functional hybrid materials based on clay minerals for enhanced electrocatalytic activity. *Journal of Alloys and Compounds*, 892, 162239.
- Tiller, R., Booth, A., Kubowicz, S., & Jahren, S. (2021). Co-production of future scenarios of policy action plans in a science-policy-industry interface-The case of microfibre pollution from waste water treatment plants in Norway. *Marine Pollution Bulletin*, 173(Pt B), 113062.
- Tu, Y., Shi, H., Zhou, X., & Lev, B. (2022). Optimal trade-off of integrated river basin water resources allocation considering water market: A bi-level multi-objective model with conditional value-at-risk constraints. *Computers & Industrial Engineering*, 169, 108160.
- Valeev, D., Bobylev, P., Osokin, N., Zolotova, I., Rodionov, I., Salazar-Concha, C., & Verichev, K. (2022). A review of the alumina production from coal fly ash, with a focus in Russia. *Journal of Cleaner Production*, 363, 132360.
- Vellingiri, B., Suriyanarayanan, A., Selvaraj, P., Abraham, K. S., Pasha, M. Y., Winster, H., Gopalakrishnan, A. V., G, S., Reddy, J. K., Ayyadurai, N., Kumar, N., Giridharan, B., P, S., Rao, K. S., Nachimuthu, S. K., Narayanasamy, A., Mahalaxmi, I., & Venkatesan, D. (2022). Role of heavy metals (copper (Cu), arsenic (As), cadmium (Cd), iron (Fe) and lithium (Li)) induced neurotoxicity. *Chemosphere*, 301, 134625.
- Vu, D.-H., Bui, H.-B., Bui, X.-N., An-Nguyen, D., Le, Q.-T., Do, N.-H., & Nguyen, H. (2020). A novel approach in adsorption of heavy metal ions from aqueous solution using synthesized MCM-41 from coal bottom ash. *International Journal of Environmental Analytical Chemistry*, 100(11), 1226–1244.
- Wang, Y., Chen, B., Xiong, T., Zhang, Y., & Zhu, W. (2022). Immobilization of U (VI) in wastewater using coal fly ash aerogel (CFAA) as a low-cost adsorbent. *Process Safety and Environmental Protection*, 160, 900–909.
- Wang, N., Hao, L., Chen, J., Zhao, Q., & Xu, H. (2018). Adsorptive removal of organics from aqueous phase by acid-activated coal fly ash: Preparation, adsorption, and Fenton regenerative valorization of “spent” adsorbent. *Environmental Science and Pollution Research International*, 25(13), 12481–12490.
- Wang, N., Jin, L., Li, C., Liang, Y., & Wang, P. (2022). Preparation of coal fly ash-based Fenton-like catalyst and its application for the treatment of organic wastewater under microwave assistance. *Journal of Cleaner Production*, 342, 130926.
- Wang, X., Sun, R., & Wang, C. (2014). pH dependence and thermodynamics of Hg (II) adsorption onto chitosan-poly (vinyl alcohol) hydrogel adsorbent. *Colloids and Surfaces A: Physicochemical and Engineering Aspects*, 441, 51–58.
- Wang, N., Sun, X., Zhao, Q., & Wang, P. (2021). Treatment of polymer-flooding wastewater by a modified coal fly ash-catalysed Fenton-like process with microwave pre-enhancement: System parameters, kinetics, and proposed mechanism. *Chemical Engineering Journal*, 406, 126734.
- Wang, N., Sun, X., Zhao, Q., Yang, Y., & Wang, P. (2020). Leachability and adverse effects of coal fly ash: A review. *Journal of Hazardous Materials*, 396, 122725.
- Wang, C., Xu, G., Gu, X., Gao, Y., & Zhao, P. (2021). High value-added applications of coal fly ash in the form of porous materials: A review. *Ceramics International*, 47(16), 22302–22315.

- Wang, Y., Yang, N., Soldatov, M., & Liu, H. (2022). A novel phosphazene-based amine-functionalized porous polymer with high adsorption ability for I2, dyes and heavy metal ions. *Reactive and Functional Polymers*, 173, 105235.
- Wang, Y., Zhang, Y., Sun, W., & Zhu, L. (2022). The impact of new urbanization and industrial structural changes on regional water stress based on water footprints. *Sustainable Cities and Society*, 79, 103686.
- Wang, N., Zhao, Q., Xu, H., Niu, W., Ma, L., Lan, D., & Hao, L. (2018). Adsorptive treatment of coking wastewater using raw coal fly ash: Adsorption kinetic, thermodynamics and regeneration by Fenton process. *Chemosphere*, 210, 624–632.
- Wassel, A. R., El-Naggar, M. E., & Shoueir, K. (2020). Recent advances in polymer/metal/metal oxide hybrid nanostructures for catalytic applications: A review. *Journal of Environmental Chemical Engineering*, 8(5), 104175.
- Wu, Y., & Ke, Z. (2022). Novel Cu-doped zeolitic imidazolate framework-8 membranes supported on copper foam for highly efficient catalytic wet peroxide oxidation of phenol. *Materials Today Chemistry*, 24, 100787.
- Xu, Z.-P., Liu, Y., Wang, S.-Y., Li, Z.-W., Lu, D.-X., Jiang, P., Pan, J., Guan, W., Kuang, H.-X., & Yang, B.-Y. (2022). Phenolic compounds of *Solanum xanthocarpum* play an important role in anti-inflammatory effects. *Arabian Journal of Chemistry*, 15(7), 103877.
- Xu, X., Zong, S., Chen, W., & Liu, D. (2019). Heterogeneously catalyzed binary oxidants system with magnetic fly ash for the degradation of bisphenol A. *Chemical Engineering Journal*, 360, 1363–1370.
- Yagub, M. T., Sen, T. K., Afroze, S., & Ang, H. M. (2014). Dye and its removal from aqueous solution by adsorption: A review. *Advances in Colloid and Interface Science*, 209, 172–184.
- Yang, L., Wang, F., Du, D., Liu, P., Zhang, W., & Hu, S. (2016). Enhanced photocatalytic efficiency and long-term performance of TiO<sub>2</sub> in cementitious materials by activated zeolite fly ash bead carrier. *Construction and Building Materials*, 126, 886–893.
- Yang, L., Wang, F., Hakki, A., Macphee, D. E., Liu, P., & Hu, S. (2017). The influence of zeolites fly ash bead/TiO<sub>2</sub> composite material surface morphologies on their adsorption and photocatalytic performance. *Applied Surface Science*, 392, 687–696.
- Yavari-Bafghi, M., Shavandi, M., Dastgheib, S. M. M., & Amoozegar, M. A. (2022). Simultaneous application of CaO<sub>2</sub> nanoparticles and microbial consortium in Small Bioreactor Chambers (SBCs) for phenol removal from groundwater. *Process Safety and Environmental Protection*, 160, 465–477.
- Yusof, M. S. M., Othman, M. H. D., Wahab, R. A., Samah, R. A., Kurniawan, T. A., Mustafa, A., Rahman, M. A., Jaafar, J., & Ismail, A. F. (2020). Effects of pre and post-ozonation on POFA hollow fibre ceramic adsorptive membrane for arsenic removal in water. *Journal of the Taiwan Institute of Chemical Engineers*, 110, 100–111.
- Zamora-Ledezma, C., Negrete-Bolagay, D., Figueroa, F., Zamora-Ledezma, E., Ni, M., Alexis, F., & Guerrero, V. H. (2021). Heavy metal water pollution: A fresh look about hazards, novel and conventional remediation methods. *Environmental Technology & Innovation*, 22, 101504.
- Zhang, S., Shi, T., Ni, W., Li, K., Gao, W., Wang, K., & Zhang, Y. (2021). The mechanism of hydrating and solidifying green mine fill materials using circulating fluidized bed fly ash-slag-based agent. *Journal of Hazardous Materials*, 415, 125625.
- Zhang, J., Yan, M., Sun, G., & Liu, K. (2021). Simultaneous removal of Cu (II), Cd (II), Cr (VI), and rhodamine B in wastewater using TiO<sub>2</sub> nanofibers membrane loaded on porous fly ash ceramic support. *Separation and Purification Technology*, 272, 118888.
- Zhang, X., Yuan, X., Yu, J., He, P., Chen, T., Zhang, L., Wang, K., Hua, X., & Zhu, P. (2022). Core@ Shell structured coal fly ash Magnetospheres@ C/g-C<sub>3</sub>N<sub>4</sub> for degradation of Rh B via photo-Fenton catalysis. *Journal of Alloys and Compounds*, 908, 164441.
- Zhao, X., Zhao, H., Huang, X., Wang, L., Liu, F., Hu, X., Li, J., Zhang, G., & Ji, P. (2021). Effect and mechanisms of synthesis conditions on the cadmium adsorption capacity of modified fly ash. *Ecotoxicology and Environmental Safety*, 223, 112550.
- Zhou, Y., Jiang, J., Qian, K., Ding, Y., Yang, S.-H., & He, L. (2021). Graph convolutional networks based contamination source identification across water distribution networks. *Process Safety and Environmental Protection*, 155, 317–324.
- Zhu, Y., Fan, W., Zhou, T., & Li, X. (2019). Removal of chelated heavy metals from aqueous solution: A review of current methods and mechanisms. *The Science of the Total Environment*, 678, 253–266.
- Zhu, L., Ji, J., Wang, S., Xu, C., Yang, K., & Xu, M. (2018). Removal of Pb (II) from wastewater using Al<sub>2</sub>O<sub>3</sub>-NaA zeolite composite hollow fiber membranes synthesized from solid waste coal fly ash. *Chemosphere*, 206, 278–284.
- Zierold, K. M., & Odoh, C. (2020). A review on fly ash from coal-fired power plants: Chemical composition, regulations, and health evidence. *Reviews on Environmental Health*, 35(4), 401–418.

**Supplemental figures and tables for paper “Coal Ash for Removing Toxic Metals and Phenolic Contaminants from Wastewater- A Brief Review”**

Abdelkader Labidi<sup>\* a</sup>, Haitao Ren<sup>a</sup>, Atif Sial<sup>a</sup>, Hui Wang<sup>a</sup>, Eric Lichtfouse<sup>b</sup>, Chuanyi Wang<sup>\* a</sup>

<sup>a</sup>School of Environmental Science and Engineering, Shaanxi University of Science and Technology, Xi’an 710021, PR China.

<sup>b</sup>Aix Marseille Univ, CNRS, IRD, INRAE, CEREGE, Aix en Provence 13100, France. Orcid: 0000-0002-8535-8073.

\*Corresponding authors

E-mail address: [abdelkaderlabidi0907@gmail.com](mailto:abdelkaderlabidi0907@gmail.com) (A. Labidi), [wangchuanyi@sust.edu.cn](mailto:wangchuanyi@sust.edu.cn) (C. Wang).

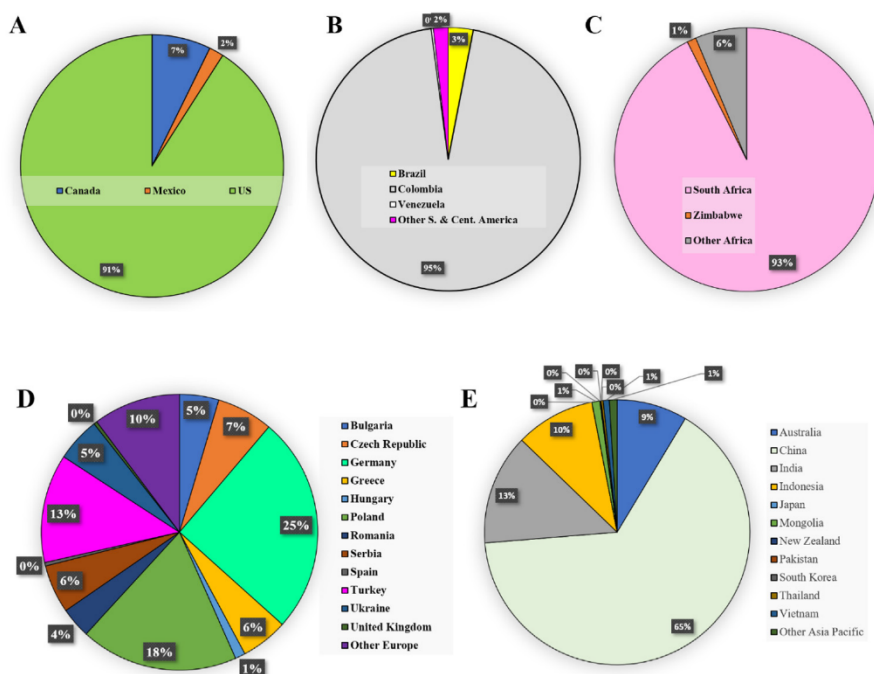


**Fig. S1.** The differences in the amount of coal production worldwide in 2018 whereas (A) Total North America, (B) Total S. & Cent. America, (C) Total CIS, (D) Total Europe and (E) Total Asia. This data is according to the Statistical Review of World Energy. Reprinted with permission of Elsevier from Alterary et al. (2021).

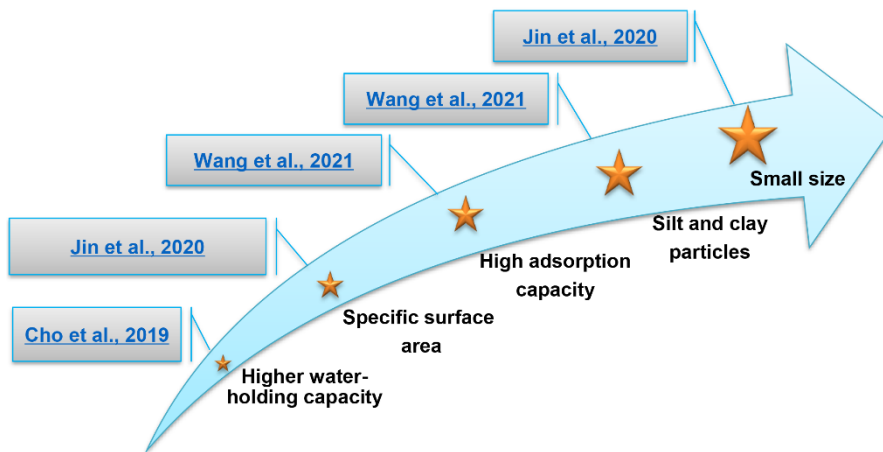


**Fig. S2.** Physiochemical properties of coal fly ash particles.

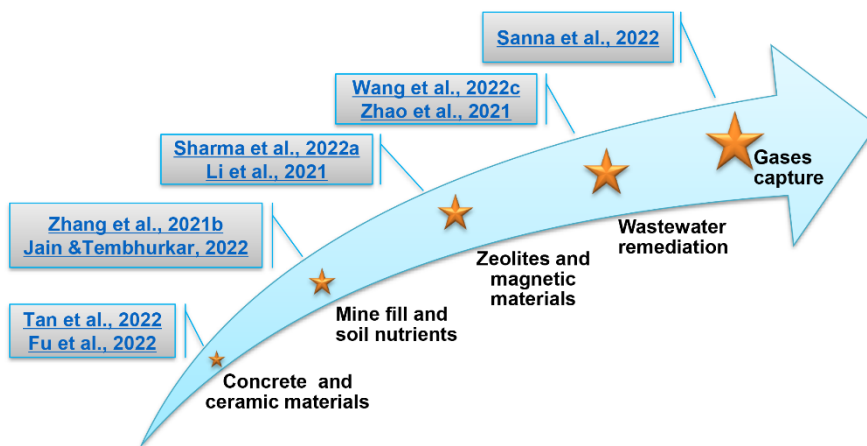


**Fig. S3.** Industrial and environmental applications of coal fly ash inorganic material.

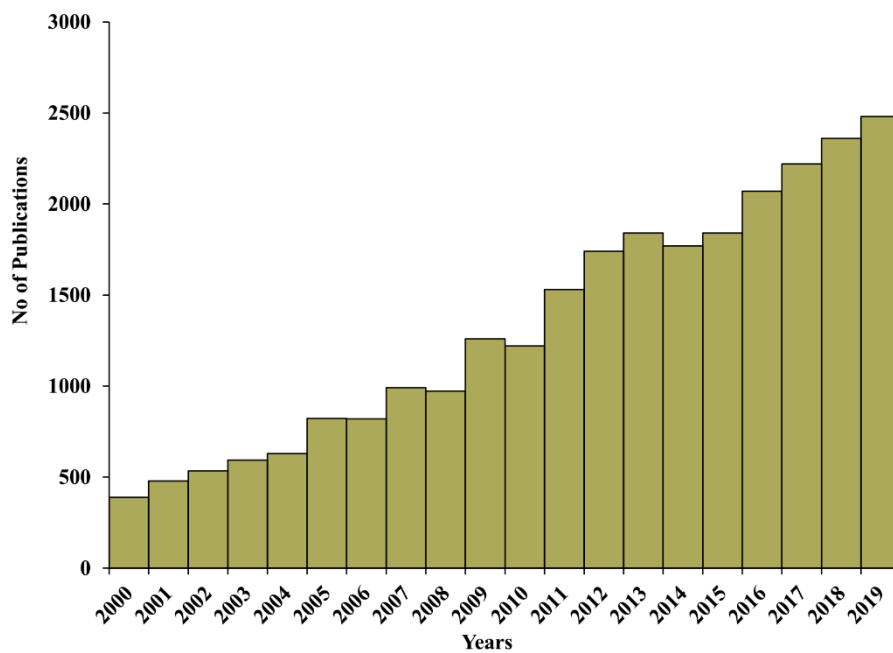


**Fig. S4.** Number of publications of fly ash per year from 2000 to 2019 according to google scholar. Reprinted with permission of Elsevier from Alterary et al. (2021).

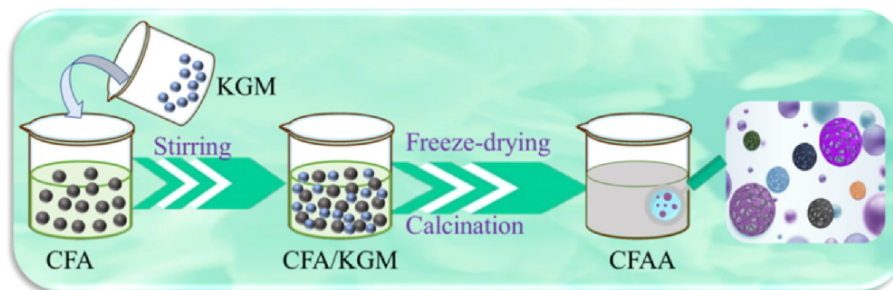


**Fig. S5.** The flow-process diagram of the synthesis of CFAA. Reprinted with permission of Elsevier from Wang et al. (2022). (CFAA): Coal fly ash acid.

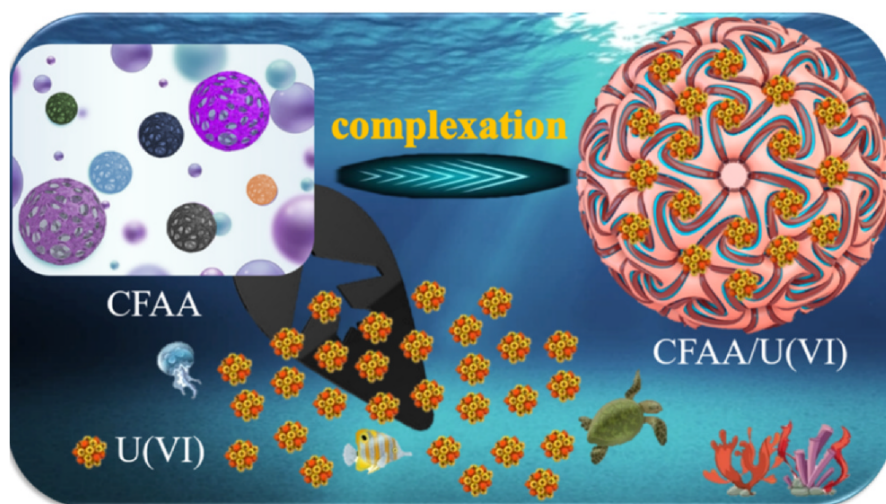


**Fig. S6.** The probable U (VI) removal mechanism by CFAA. Reprinted with permission of Elsevier from Wang et al. (2022). (CFAA): Coal fly ash acid.

**Table S1.** Examples of coal ash-based adsorbents for heavy metals and phenolic compounds adsorption.

Adsorbent material	Preparation method	Analysis Techniques	Pollutants	Conditions	R <sup>a</sup> (%) or Q <sub>max</sub> <sup>b</sup> (mg. g <sup>-1</sup> )	Adsorption isotherms	Refs
Coal fly ash aerogel (CFAA)	Calcination-freeze-drying technology	SEM, FTIR, XRD and XPS	U (VI)	$C_0 = 10 \text{ mg. L}^{-1}$ , $m_{ads} = 1.0 \text{ g L}^{-1}$ , $T = 298 \text{ K}$ , $t = 24 \text{ h}$ and $pH = 3.0$	94.5 % 110.7 mg. g <sup>-1</sup>	Langmuir and Freundlich	(Wang et al., 2022)
Coal fly ash-(NaOH)	Low-temperature hydrothermal	SEM-EDS, FTIR, XRD, and XPS	Cd (II)	$m_{ads}=0.1 \text{ g L}^{-1}$ , $C_0= 100 \text{ mg. L}^{-1}$ , $T= 318 \text{ K}$ , $t= 120 \text{ min}$ and $pH= 4.0$	90.2 mg. g <sup>-1</sup>	Langmuir, Freundlich and Temkin	(Zhao et al., 2021)
Low alumina fly ash (LAFA)	Alkali fusion method and wet impregnation	TEM, SEM, FTIR, XRD and XPS	As (III) and As (V)	$m_{ads}= 2.0 \text{ g. L}^{-1}$ , $pH= 10$ and $8.5$ respectively, $T=293 \text{ K}$ and $t=12 \text{ h}$	2725 µg of As(V)/g and 2281.9 µg of As(III)/g	Langmuir and Freundlich	(Min et al., 2021)
Alkali fly ash	Microwave-assisted alkali-modification	SEM, TEM and X-ray fluorescence	Hg (II)	$m_{ads}= 0.5 \text{ g. L}^{-1}$ , $T= 25 \text{ }^\circ\text{C}$ , $t= 90 \text{ min}$ and $C_0= 10 \text{ mg L}^{-1}$	2.6 mg. g <sup>-1</sup>	Langmuir and Freundlich	(Qi et al., 2019)
Zeolites prepared from coal fly ash	Hydrothermal treatment	XRD, XRF, SEM and N <sub>2</sub> adsorption	Pb (II), Cd (II), Cu (II), Zn (II) and Co (II)	$C_0= 200 \text{ mg. L}^{-1}$ , and $t = 200 \text{ min}$	103.0, 74.0, 57.8, 42.0 and 30.2 mg. g <sup>-1</sup>	Langmuir	(Joseph et al., 2020)
Dithizone-coal bottom ash	Immobilization method	FTIR, SEM-EDX, TEM, XRD, DSC/TGA	Pb (II)	$C_0=20 \text{ mg. L}^{-1}$ $pH= 4.01$ and $t = 90 \text{ min}$	31.25 mg. g <sup>-1</sup>	Langmuir, Freundlich, Temkin and Dubinin-Radushkevich	Huda et al., 2021
Bottom fly ash	Alkali synthesis	FTIR, SEM, XRD NMR, TEM,	Pb <sup>2+</sup> , Cu <sup>2+</sup> and Cd <sup>2+</sup>	$m_{ads}= 1.67 \text{ g L}^{-1}$ , $T= 25 \text{ }^\circ\text{C}$ , $t= 12\text{h}$ , $pH= 5$ and $C_0=100 \text{ mg. L}^{-1}$	99.4 %, 41.66 %, and 43.98 %	Langmuir and Freundlich	Vu et al., 2020
Cationic PDDA-FA	Ultrathin coating layer by layer	SEM-EDX, FTIR, Raman and TGA	Phenol	$m_{ads}=5.0 \text{ g. L}^{-1}$ $C_0=5.0 \text{ mg. L}^{-1}$ , $pH=7.0$ , room temperature and $t=2.0\text{h}$	95 %	Langmuir, Freundlich and Temkin	(Oyehan et al., 2020)
Fly-ash-cenospheres/Fe <sub>3</sub> O <sub>4</sub>	Co-precipitation technique	FTIR, TGA, SEM and XRD	NP, (2,4-DCP), (BPA), (MDP), (PTOP)	$C_0= 100 \text{ mg. L}^{-1}$ , $pH= 6.0$ , $m_{ads}=1.0 \text{ g. L}^{-1}$ , and $T= 25^\circ\text{C}$	434.8 mg. g <sup>-1</sup>	Langmuir and Freundlich	(Pan et al., 2013)
South African coal fly ash (SACFA)	Electrostatic precipitation	XRF, XRD and N <sub>2</sub> adsorption	4-NP, 2-NP and phenol	$C_0= 20 \text{ mg. L}^{-1}$ , $t= 360 \text{ min}$ and $pH= 2.22$	92.6 %, 90.2 % and 88.9 %	Langmuir and Freundlich	(Bada et al., 2013)

Agricultural waste Bagasse Fly Ash (BFA) (MMZBFA)	Electrolyte supported microwave hydrothermal treatment	XRF, PXRD, SEM and FTIR	Ortho-chlorophenol	$pH\ 7.0, C_0=150\ mg.\ L^{-1}, m_{ads}=1\ g.\ L^{-1}, t=120\ min, T:$ room temperature	$31.9\ mg.\ g^{-1}$	Langmuir, Freundlich, Dubinin-Radushkevich and Temkin	(Shah et al., 2017)
Activated CFA	Acid-based activation	BET and SEM	P-nitrophenol	$m_{ads}=2.0\ g.\ L^{-1}, T=30\ ^\circ C, t=120\ min, pH=6.5, C_0=25\ mg.\ L^{-1}$	85.6 %	NA	(Wang et al., 2018)

TEM: Transmission electron microscopy, SEM: Scanning electron microscope, SEM-EDS: Scanning electron microscope-Energy dispersive X-ray spectroscopy, FTIR: Fourier-transform infrared spectroscopy, XRD: X-ray diffraction, XPS: X-ray photoelectron spectroscopy, DSC/TGA: Differential scanning calorimetry/ Thermogravimetric analysis, ICP-AES: Inductively coupled plasma atomic emission spectroscopy, XRF: X-ray fluorescence spectroscopy, PXRD: Powder X-Ray diffraction, NMR: solid-state nuclear magnetic resonance, NP: Nitrophenol, 2, 4-DCP: 2, 4-dichlorophenol, MDP: 3,4-(methylenedioxy)phenol, BPA: Bisphenol A, PTOP: p-(tert-octyl)phenol,  $m_{ads}$ : Mass of adsorbent,  $C_0$ : Initial concentration, PDDA-FA: Polydiallyldimethyl ammonium chloride-fly ash, CFA: Coal fly ash,  $R^a$ : Percent removal (%) or  $Q_{max}$ : maximum adsorption capacity,  $b$ : the value of the maximum adsorption capacity corresponds to the Langmuir isotherm, NA: Not available.

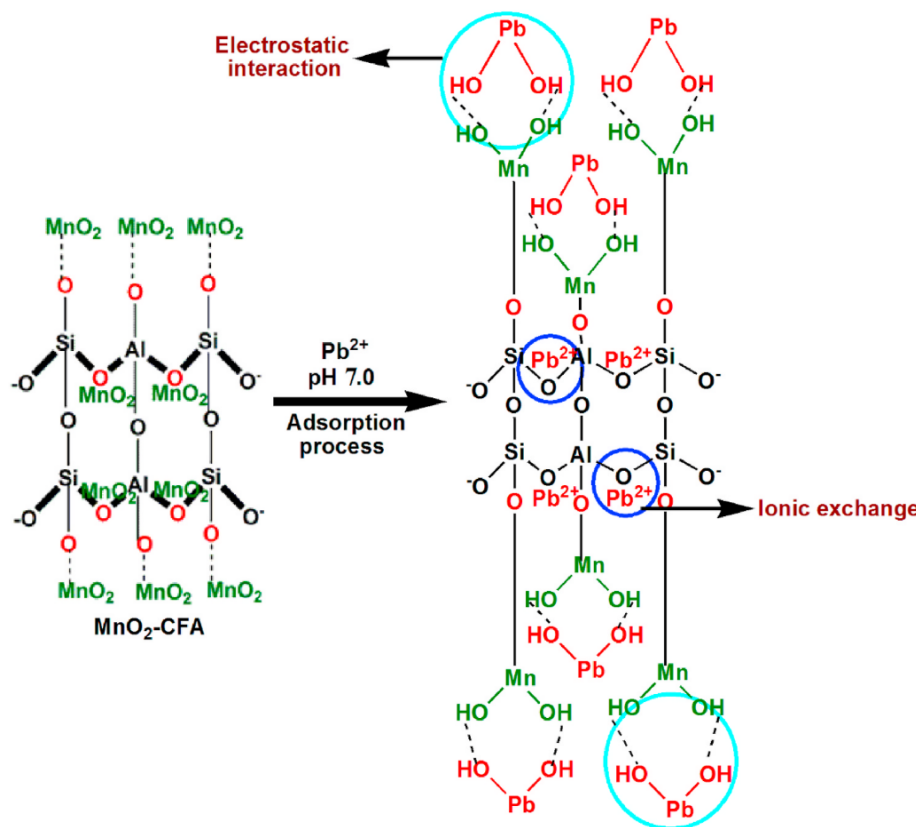


**Fig. S7.** Proposed mechanism of  $Pb^{2+}$  adsorption using  $MnO_2$ -CFA. Reprinted with permission of Elsevier from Mofulatsi et al. (2022). (CFA): Coal fly ash.

### Text S3.2.1

The nonlinear pseudo-first-order model is described as shown by (Eq. 1)(Repo, 2011):

$$\frac{dq}{dt} = K_1(q_e - q_t) \quad (1)$$

while linear version of the pseudo-first-order model is presented by Lagergren as follows (Eq. 2):

$$\log(q_e - q_t) = \log q_e - \frac{K_1}{2.303} t \quad (2)$$

where  $q_e$  and  $q_t$  are the adsorption capacities of each residue ( $\text{mg. g}^{-1}$ ) at equilibrium and at any time ( $t$ ) respectively and  $K_1$  ( $\text{min}^{-1}$ ) denotes the adsorption constant. The plot of  $\log(q_e - q_t)$  against time ( $t$ ) was used to determine the constant ( $K_1$ ) values of each residue removal.

The nonlinear pseudo-second-order rate equation is written below (Eq. 3)(Repo, 2011):

$$\frac{dq}{dt} = K_2(q_e - q_t)^2 \quad (3)$$

The linear form of the pseudo-second-order rate equation of McKay and Ho is expressed by (Eq. 4):

$$\frac{t}{q_t} = \frac{1}{k_2 q_e^2} + \frac{1}{q_e} t \quad (4)$$

where  $k_2$  is the pseudo-second-order rate constant ( $\text{g. mmol}^{-1} \cdot \text{min}^{-1}$ ). The plot of the variation of  $\left(\frac{t}{q_t}\right)$  vs. ( $t$ ) allows determining the constant  $K_2$ .

The external diffusion model is expressed as follow (Eq.5)(An et al., 2016; Repo, 2011):

$$\frac{dC_t}{dt} = K_s s(C_t - C_s) \quad (5)$$

where  $C_s$  and  $C_t$  are respectively the concentrations of solute on the surface and in solution ( $\text{mg. L}^{-1}$ ),  $K_s$  represents the mass transfer constant and ( $s$ ) denotes the specific surface area of the adsorbent.

The intra-particle model can be expressed in the following form (Eq. 6)(Mofulatsi et al., 2022):

$$q_t = k_p t^{1/2} + C \quad (6)$$

where  $k_p$  ( $\text{mg g}^{-1} \text{min}^{-1/2}$ ) is the constant of intra-particle diffusion model and  $C$  ( $\text{mg. g}^{-1}$ ) corresponds to a constant related to the thickness of the boundary layer. The variation of the curve of  $q_t = f(t^{1/2})$  at various concentrations of each residue allows determining the controlled adsorption process parameters.

### Text S3.2.2

The Langmuir isotherm shows that the adsorbent sites in surface have identical energy and each pollutant is situated on a single site. It shows the formation of the monolayer of the adsorbate covering a homogeneous adsorbent surface (An et al., 2016; Buema et al., 2021; Repo, 2011).

The Langmuir nonlinear equation applied in a single pollutant system is given by (Eq. 7) (An et al., 2016; Repo, 2011):

$$q_e = \frac{K_l q_m C_e}{1 + K_l C_e} \quad (7)$$

The linear form of Langmuir equation used in a single pollutant system is presented by (Eq.8)(An et al., 2016; Repo, 2011):

$$\frac{C_e}{q_e} = \frac{1}{q_m k_l} + \frac{C_e}{q_m} \quad (8)$$

where  $q_e$  is the amount of the residue adsorbed per unit mass of the adsorbent (mg. g<sup>-1</sup>),  $C_e$  designates the concentration of residue in the equilibrium solution (mg. L<sup>-1</sup>),  $q_m$  represents the maximum adsorption capacity (mg. g<sup>-1</sup>), and  $k_l$  denotes the Langmuir adsorption constant (L. mg<sup>-1</sup>). The dimensionless constant ( $R_l$ ) (Eq.9) of Langmuir is generally applied to indicate the feasibility of the adsorption process and the interaction between the adsorbent and each pollutant. The value of separation factor ( $R_l$ ) demonstrates whether the shape of the Langmuir model is unfavourable ( $R_l > 1$ ), linear ( $R_l = 1$ ), favorable, ( $0 < R_l < 1$ ) and irreversible ( $R_l = 0$ ) (Mofulatsi et al., 2022; Repo, 2011).

$$R_l = \frac{1}{K_l C_0 + 1} \quad (10)$$

On the one hand, Freundlich model is an empirical isotherm appropriate to multilayer adsorption on heterogeneous sites in the adsorbent surface (Nebaghe et al., 2016; Repo, 2011). The nonlinear form of Freundlich equation is given by (Eq. 11) (Nebaghe et al., 2016; Repo, 2011):

$$q_e = K_F C_e^{\frac{1}{n}} \quad (11)$$

The above equation can be linearized as (Eq. 12):

$$\log q_e = \log K_f + \frac{1}{n} \log C_e \quad (12)$$

where  $q_e$  is the equilibrium pollutant concentration on the adsorbent (mg g<sup>-1</sup>),  $C_e$  refers to the equilibrium concentration of each pollutant in the solution (mg. L<sup>-1</sup>),  $K_F$  (mg. g<sup>-1</sup>) / (L/g)<sup>n</sup>, and  $n$  represents the Freundlich constant that describes the isotherm nonlinearity. On the other hand, The MLF (combined Langmuir and Freundlich isotherms) is a three-parameter empirical equation frequently applied to model the adsorption equilibrium data. Thus, in this isotherm, there is linear dependency on the mass of pollutant in the numerator and exponentially in the denominator to enhance the wide range

of the concentration of adsorption equilibrium data. The nonlinear equation can be expressed as follows (Eq. 13):

$$q_e = \frac{q_{mon} K_{MLF} C_e^{\frac{1}{n}}}{1 + K_{MLF} C_e^{\frac{1}{n}}} \quad (13)$$

However, the linearized (MLF) model is presented by (Eq. 14):

$$\ln \left( \frac{q_e}{q_{mon} - q_e} \right) = \frac{1}{n} \ln C_e + \ln (K_{MLF})^{\frac{1}{n}} \quad (14)$$

where  $q_{mon}$  is the adsorption capacity ( $\text{mg. g}^{-1}$ ), while  $K_{MLF}$  ( $\text{L. mg}^{-1}$ ) and  $n$  are the MLF constants. The value of  $\frac{1}{n}$  lays between zero and unity.

Other isotherms were widely applied to study adsorption data such as Temkin isotherm which assumes that the adsorption heat of all molecules decreases linearly with the increase in the coverage of adsorbent surface (Nebaghe et al., 2016). The nonlinear Temkin's equation is written below (Eq. 15) (Nebaghe et al., 2016):

$$q_e = \frac{RT}{b_T} \ln (K_T C_e) \quad (15)$$

The linear Temkin's equation is formulated in (Eq. 16):

$$q_e = \frac{RT}{b_T} \ln K_T + \frac{RT}{b_T} \ln C_e \quad (16)$$

Where  $q_e$  is the equilibrium of each pollutant concentration on the adsorbent ( $\text{mg. g}^{-1}$ ),  $C_e$  designates the equilibrium concentration of each pollutant in the solution ( $\text{mg. L}^{-1}$ ), while  $K_T$  ( $\text{L. g}^{-1}$ ) and  $b_T$  are the Temkin constants.

Dubinin-Radushkevich (R-D) isotherm model widely applied to describe adsorption data. Unlike the Langmuir isotherm, this model does not indicate a homogeneous surface of adsorbents or a constant adsorption potential and used to demonstrate the porous structure of adsorbents (Nebaghe et al., 2016; Repo, 2011). It is defined by the following equation (Eq. 17) (Nebaghe et al., 2016; Repo, 2011):

$$q_e = q_m e^{-B_{DR} \varepsilon^2} \quad (17)$$

The linearized Dubinin-Radushkevich (R-D)'s model represented by (Eq. 18):

$$\ln q_e = \ln q_m - B_{DR} \varepsilon^2 \quad (18)$$

where  $\varepsilon$  is the Polanyi potential and  $B_{DR}$  ( $\text{mmol}^2 \cdot \text{J}^{-2}$ ) is related to the mean free energy of the adsorption per molecule when it is transferred to the surface from infinity of the bulk phase.

The Redlich-Peterson isotherm suggests a three parameters adsorption and can be applied to both homogeneous and heterogeneous adsorption systems (Repo, 2011; Tahari et al., 2021). This empirical model connects elements from Langmuir and the Freundlich isotherm without ideal monolayer adsorption. The nonlinear equation can be expressed as follows (Eq. 19) (Nebaghe et al., 2016; Repo, 2011):

$$q_e = \frac{K_{RP} C_e}{1 + A_{RP} C_e^\alpha} \quad (19)$$

On the other hand, the linearized Redlich-Peterson isotherm equation is written as follows (Eq.20):

$$\ln \left( \frac{C_e}{q_e} \right) = \alpha \ln C_e - \ln k_{RP} \quad (20)$$

where  $K_{RP}$  ( $\text{g}^{-1}$ ) and  $A_{RP}$  ( $\text{mg} \cdot \text{L}^{-1}$ ) $^{-\alpha}$  are the Redlich-Peterson constants,  $\alpha$  is the dimensionless exponent whose value varies between 0 and 1.0 and  $C_e$  denotes the equilibrium concentration of each pollutant in the solution ( $\text{mg L}^{-1}$ ).

The linear regression coefficient ( $R^2$ ) is usually used to compare the linear and non-linear data and sum of squared estimate of errors (SSE) are usually calculated in the adsorption equilibrium data (Eq. 21). They are frequently applied in order to find the best isotherm model and kinetic models for the linear and nonlinear forms of different isotherms and kinetic models. SSE is given by the following equation (Dogar et al., 2020).

$$SSE = \sum_{i=1}^m (q_{e,cal} - q_{e,exp})^2 \quad (21)$$

Moreover, heavy metals phenolic compounds adsorption can be investigated in single system (one pollutant in solution) as well as in multisystem which contains more than one pollutant in solution. For example, it is essential to explore the aptitude of coal fly ash based-materials towards two pollutants (binary system) to examine the affinity and the selectivity of these inorganic materials in removing

different pollutants in the solution. Their equilibrium capacities using different models are given in the following equations (Eqs. (22-25), Repo, 2011).

$$q_{e1} = \frac{K_{l1,1}q_{m1}C_{e1}}{1 + K_{l1,1}C_{e1} + K_{l1,2}C_{e2}} \quad (22)$$

$$q_{e2} = \frac{K_{l1,2}q_{m2}C_{e1}}{1 + K_{l1,1}C_{e1} + K_{l1,2}C_{e2}} \quad (23)$$

$$q_{e1} = \frac{K_{RP1}C_e}{1 + A_{RP1}C_{e1}^{\alpha1} + A_{RP2}C_{e2}^{\alpha2}} \quad (24)$$

$$q_{e2} = \frac{K_{RP2}C_e}{1 + A_{RP1}C_{e1}^{\alpha1} + A_{RP2}C_{e2}^{\alpha2}} \quad (25)$$

where  $q_{e1}$  and  $q_{e2}$  are the amounts of components 1 and 2 adsorbed on the surface of adsorbent at equilibrium,  $q_{m1}$  and  $q_{m2}$  represent their maximum adsorption capacities,  $K_{l1,1}$  and  $K_{l1,2}$  designate respectively the affinity constants of the used adsorbent towards the components 1 and 2, while  $C_{e1}$  and  $C_{e2}$  correspond to the residual concentrations of the components in the solution at equilibrium. Furthermore, other empirical models were reported in the literature for pollutants removal in binary system led to get insight into the adsorption behavior especially to more understand the mechanism of each residue removal (Repo, 2011; Tahari et al., 2021).

**Table S2.** Examples of coal ash-based membranes for heavy metals and phenolic compounds separation.

Membrane material	Preparation method	Analysis Techniques	Pollutants	Separation Conditions	R <sup>a</sup> (%) or Q <sub>max</sub> (mg. g <sup>-1</sup> )	Pollutants detection	Refs.
Al <sub>2</sub> O <sub>3</sub> -NaA hollow fiber membranes	Hydrothermal method	SEM and XRD	Pb (II)	$C_0 = 50 \text{ mg. L}^{-1}$ , 0.1 MPa trans-membrane pressure, $T = 25^\circ\text{C}$ , filtration time = 12h	>99 %	ICP-OES	(Zhu et al., 2018)
TiO <sub>2</sub> nanofibers membrane loaded on porous fly ash	Hydrothermal method	XRD, EDS, SEM and TEM	Cu (II), Cd (II) and Cr (VI)	Water flux = 223 L. m <sup>-1</sup> . h <sup>-1</sup> . bar <sup>-1</sup> , $t = 240 \text{ min}$ , $C_0 = 100 \text{ mg. L}^{-1}$ of each Cu(II), Cd(II) and Cr(VI) respectively	Cd(II)=341.53 %, Cu(II)= 90.15 %, Cr(VI)= 97.09 % Cu(II)= 9.56 mg. g <sup>-1</sup> , Cd(II) = 4.72 mg. g <sup>-1</sup> , Cr(VI) = 6.65 mg. g <sup>-1</sup>	ICP-OES, UV spectrophotometer	(Zhang et al., 2021)
Fly Ash Composite Membrane	Ultrasonication	FTIR, SEM and contact angle	Phenol	$C_0 = 100 \text{ mg. L}^{-1}$ , applied pressure: 207 kPa, pH = 10 and water flux = 1.86 L. m <sup>-2</sup> . h <sup>-1</sup>	97,2 %	UV-Vis spectrophotometer	(Gupta et al., 2020)
Porous and flexible membrane	Layer by layer assembly	XRD, XPS, BET, FTIR, SEM and TGA	Pb (II)	$C_0 = 100 \text{ ppm}$ , pH= 5.2 $m_{\text{membrane}} = 0.0675 \text{ g}$ , injection = 0.1 mL. m <sup>-1</sup>	1443.29 mg. g <sup>-1</sup>	ICP-OES	(Huang et al., 2020)
PVA-ceramic composite membrane	Crosslinking	SEM and contact angle	Phenol	Applied pressure = 207 kPa, $C_0 = 200 \text{ mg. L}^{-1}$ , pH=6.0	85 %	4aminoantipyrrene method	(Gupta & Anandkumar, 2019)
Fluidized bed fly ash (CFBFA)	Co-polymerization/hydrothermal	XRF, XRD, FTIR, SEM, BET, TGA/DSC and ζ-potential	Cr (VI)	Applied pressure = 10 kPa, pH=7.0, $C_0 = 1000 \text{ mg. L}^{-1}$	85.45 %	ICP-OES, UV-Vis spectrophotometer	(He et al., 2020)
POFA hollow fibre ceramic adsorptive membrane	Combined phase inversion and sintering technique	Raman, BET, TGA, FTIR, AFM and XRD	As (III) and As (V)	Mechanical strength = 52.84 MPa, water flux = 250.73 L. m <sup>-2</sup> .h <sup>-1</sup> , $C_0 = 100 \text{ ppm}$	95.62 and 98.34 mg. g <sup>-1</sup>	ICP-OES	(Yusof et al., 2020)
Fly ash - kaolin	Combination method	TGA, XRD and SEM	Humic acid	Mechanical strength= 43.6MPa, $C_0 = 50 \text{ mg. L}^{-1}$ , $t = 20 \text{ min}$	98.46%	UV-Vis spectrophotometer	(Rawat and Bulasara, 2018)

R<sup>a</sup>: Percent removal (%), TEM: Transmission electron microscopy, SEM: Scanning electron microscopy, SEM-EDS: Scanning electron microscope-Energy dispersive X-ray spectroscopy, FTIR: Fourier-transform infrared spectroscopy, XRD: X-ray diffraction, XPS: X-ray photoelectron spectroscopy, DSC/TGA: Differential scanning calorimetry/ Thermogravimetric analysis, ICP-OES: Inductively coupled plasma atomic emission spectroscopy, XRF: X-ray fluorescence spectroscopy, ζ-potential: Zeta potential, PVA: polyvinylalcohol.

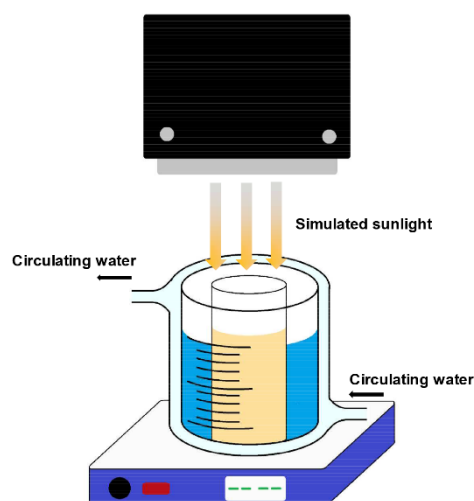


**Fig. S8.** Experimental setup for the photochemical reaction experiments. Reprinted with permission of American Chemical Society (ACS) from Fu et al. (2018).

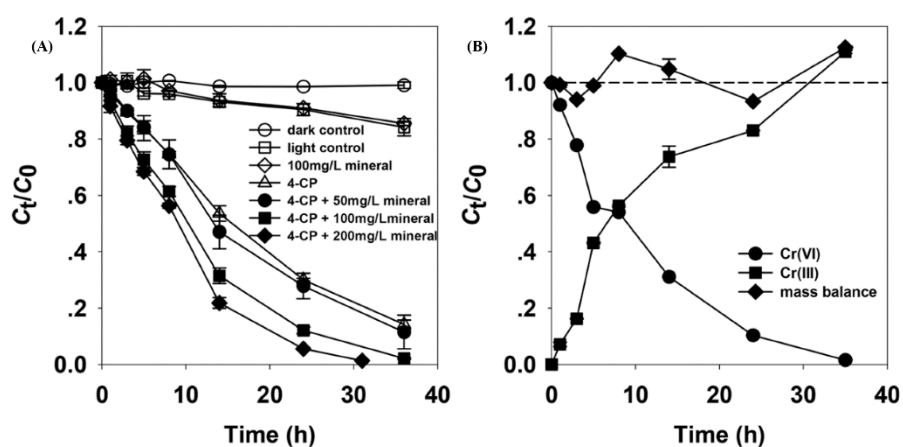


**Fig. S9.** (A) Concentration-time profiles of Cr(VI) in different reaction systems and (B) mass balance of Cr species in the ternary system under simulated sunlight. Reaction conditions: 0.2 mM Cr(VI) and 0.3 mM 4-chlorophenol (4-CP) or 0-200 mg L<sup>-1</sup> dissolved mineral ash in 40 mM phosphate buffer (pH 4.7 ± 0.1) at 20 °C. Dark control and mass balance were examined in solution containing 0.2 mM Cr(VI), 0.3 mM 4-CP, and 100 mg L<sup>-1</sup> mineral. Error bars represent ± one standard deviation from the mean of triplicate samples. Reprinted with permission of American Chemical Society (ACS) from Fu et al. (2018).

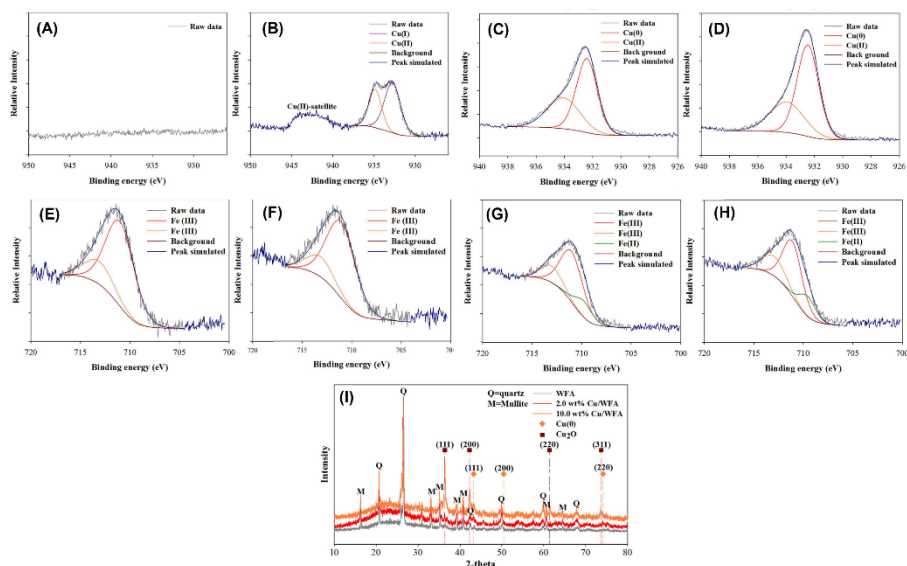


**Fig. S10.** XPS spectra for the narrow scan of Cu (2p) (0.25 wt. %) and Fe (2p<sub>3/2</sub>) on the surface of (A and E) WFA, (B and F) Cu/WFA before and (C and G) after activation, and (D and H) after reaction. XRD patterns of WFA support, 2 wt. % and 10 wt. % Cu/WFA (I). Reprinted with permission of Elsevier from Park et al. (2020).

XPS: X-ray photoelectron spectroscopy, XRD: X-ray diffraction, FESEM: Field emission scanning electron microscope, WFA: Water washed coal fly ash.

**Table S3.** Examples of coal ash-based photocatalysts for heavy metals and phenolic compounds photodegradation.

Photocatalyst materials	Preparation methods	Analysis Techniques	Pollutants	Conditions	R <sup>a</sup> (%)	Pollutants detection	Refs.
Mineral Ash Generated by Vegetation Fire	Pyrolyzing bamboo biomass	XRF, XRD, ζ-potential and DLS	Cr (VI)	0.2 mM Cr (VI), pH higher than 5.6, [Catalyst]= 100 mg. L <sup>-1</sup> and 200 mg. L <sup>-1</sup> , in the presence of 0.3 mM 4-chlorophenol, 14 h irradiation time	80 %	DPC colorimetric method	(Fu et al., 2018)
Ceramsite particles (CPs) containing flay ash	High-speed rotary crusher	XRD, SEM, EDS and N <sub>2</sub> adsorption	Cr (VI)	C <sub>0</sub> = 400 mg L <sup>-1</sup> , 4424 mg. L <sup>-1</sup> (citric acid), and [Catalyst]= 2.0 g. L <sup>-1</sup> , pH = 2.6, time = 9.0 d T= 30 <sup>o</sup> C	98.9 %	Atomic absorption spectrophotometer	(Cao et al., 2021)
Fe (0) catalyst on NaOH-treated coal fly ash	Impregnation method	SEM-EDS, XRD, XPS and BET	P- nitrophenol (P-NP)	C <sub>0</sub> = 0.1 mL (0,1 mM), [Catalyst]= 1.0 mg, 0.9 mL of DIW and 1.0 mL of NaBH <sub>4</sub> (150 mM), T= 25 ± 0.2 <sup>o</sup> C	100 %	HPLC, UV-Vis spectrometry	(Kim and Bae, 2018)
Cu loading on Fe sites of fly ash	Water-washed coal fly ash (WFA)	HR-FESEM, EDS, XRD and XPS	P-nitrophenol (P-NP)	[Catalyst] = 1.2 mg, 1.9 mL of DIW, C <sub>0</sub> = 0.1 Mm, 50 mM NaBH <sub>4</sub> , t=10 min, T=25 <sup>o</sup> C	100 %	UV-vis spectrophotometer	(Park et al., 2020)
H <sub>2</sub> O <sub>2</sub> /peroxydisulfate-magnetite-coal fly ash	Co-precipitation	XPS, FE-SEM, TEM, XRD and VSM	Bisphenol A	C <sub>0</sub> = 50 mg. L <sup>-1</sup> , t = 60 min, [oxidants] <sub>0</sub> = 20 mM, [H <sub>2</sub> O <sub>2</sub> ]/[PDS] <sub>0</sub> = 4, [Catalyst] = 2.0 g. L <sup>-1</sup> , pH = 5.0, T = 25 <sup>o</sup> C	100 %	UPLC	(Xu et al., 2019)
Pd catalyst supported by iron-rich fly ash@fly ash-SiO <sub>2</sub>	Impregnation	HR-FESEM, EDS, XRD, XPS, BET and ζ-potential	P-nitrophenol (P-NP)	[Catalyst]= 0.20 g. L <sup>-1</sup> -, 50-mM of p-NP and NaBH <sub>4</sub> , pH > 11, t=1.0 min	100 %	HPLC, UV-vis spectrophotometer	(Park and Bae, 2019)
Nano CuO immobilized fly ash zeolite Fenton-like catalyst	Hydrothermal	AAS, XRD, FTIR, HR-SEM and BET	P-nitrophenol and P-nitroaniline	[Catalyst]=500 mg. L <sup>-1</sup> , 20 ppm PNP and PNA, pH = 6.5, 2.0 mL of H <sub>2</sub> O <sub>2</sub> , room temperature, t= 180 min	96 and 84 %	HPLC	Subbuleks hmi and Subramanian, 2017 )

TEM: Transmission electron microscopy, SEM: Scanning electron microscopy, HRSEM: High resolution scanning electron microscopy, EDS: Energy dispersive X-ray spectroscopy, SEM-EDS: Scanning electron microscope-Energy dispersive X-ray spectroscopy, FTIR: Fourier-transform infrared spectroscopy, XRD: X-ray diffraction, XPS: X-ray photoelectron spectroscopy, FESEM: Field emission scanning electron microscope, HR-FESEM: High resolution field emission scanning electron microscope DLS: Dynamic light scattering, BET: Brunauer-Emmett-Teller, XRF: X-ray fluorescence spectroscopy, VSM: Vibrating sample magnetometer, HPLC: High performance liquid chromatography, DPC: Diphenylcarbazine, UPLC: Ultra-performance liquid chromatography, AAS: Atomic absorption spectrophotometry, UV-Vis: ultraviolet visible spectrophotometer: Ultraviolet-visible spectrophotometer, ζ-potential: Zeta potential, PNP: p-nitrophenol, <sup>a</sup>R: Percent removal (%).

## References

1. Alterary, S.S., & Marei, N.H. (2021). Fly ash properties, characterization, and applications: A review. *Journal of King Saud University Science*, 33, 101536. <https://doi.org/10.1016/j.jksus.2021.101536>.
2. An, C., Yang, S., Huang, G., Zhao, S., Zhang, P., & Yao, Y. (2016). Removal of sulfonated humic acid from aqueous phase by modified coal fly ash waste: equilibrium and kinetic adsorption studies. *Fuel*, 165, 264-271. <https://doi.org/10.1016/j.fuel.2015.10.069>.
3. Bada, S., Potgieter, J., & Afolabi, A. (2013). Kinetics studies of adsorption and desorption of South African fly ash for some phenolic compounds. *Particulate Science and Technology*, 31,1-9. <https://doi.org/10.1080/02726351.2011.613897>.
4. Buema, G., Lupu, N., Chiriac, H., Ciobanu, G., Bucur, R.-D., Bucur, D., Favier, L., & Harja, M. (2021). Performance assessment of five adsorbents based on fly ash for removal of cadmium ions. *Journal of Molecular Liquids*, 333, 115932. <https://doi.org/10.1016/j.molliq.2021.115932>.
5. Cao, J., Cui, Z., Wang, T., Zou, Q., Zeng, Q., Luo, S., Liu, Y., & Liu, B. (2021). Reductive removal of Cr (VI) by citric acid promoted by ceramsite particles: Kinetics, influential factors, and mechanisms. *Material Today Communications*, 28, 102716. <https://doi.org/10.1016/j.mtcomm.2021.102716>.
6. Fu, H., Zhou, Z., Zheng, S., Xu, Z., Alvarez, P.J., Yin, D., Qu, X., & Zhu, D. (2018). Dissolved mineral ash generated by vegetation fire is photoactive under the solar spectrum. *Environmental Science & Technology*, 52, 10453-10461. <https://doi.org/10.1021/acs.est.8b03010>.
7. Gupta, V., & Anandkumar, J. (2019). Synthesis of crosslinked PVA-ceramic composite membrane for phenol removal from aqueous solution. *Journal of the Serbian Chemical Society*, 84, 211-224. <https://doi.org/10.2298/JSC180424083G>.
8. Gupta, V., Raja, C., & Anandkumar, J. (2020). Phenol Removal by Novel Choline Chloride Blended Cellulose Acetate-Fly Ash Composite Membrane. *Periodica Polytechnica Chemical Engineering*, 64, 116-123. <https://doi.org/10.3311/PPch.14126>.
9. He, P.Y., Zhang, Y.J., Chen, H., Han, Z.C., & Liu, L.C. (2020). Low-cost and facile synthesis of geopolymer-zeolite composite membrane for chromium (VI) separation from aqueous solution. *Journal of Hazardous Materials*, 122359. <https://doi.org/10.1016/j.jhazmat.2020.122359>.
10. Huang, L., Wu, B., Wu, Y., Yang, Z., Yuan, T., Alhassan, S.I., Yang, W., Wang, H., & Zhang, L. (2020). Porous and flexible membrane derived from ZIF-8-decorated hyphae for outstanding adsorption of Pb<sup>2+</sup> ion. *Journal of Colloid and Interface Science*, 565, 465-473. <https://doi.org/10.1016/j.jcis.2020.01.035>.
11. Huda, B.N., Wahyuni, E.T., Mudasir, M., 2021. Eco-friendly immobilization of dithizone on coal bottom ash for the adsorption of lead (II) ion from water. *Results in Engineering*, 10, 100221. <https://doi.org/10.1016/j.rineng.2021.100221>.
12. Joseph, I.V., Tosheva, L., & Doyle, A.M. (2020). Simultaneous removal of Cd (II), Co (II), Cu (II), Pb (II), and Zn (II) ions from aqueous solutions via adsorption on FAU-type zeolites prepared from coal fly ash. *Journal of Environmental Chemical Engineering*, 8, 103895. <https://doi.org/10.1016/j.jece.2020.103895>.
13. Kim, M., & Bae, S. (2018). Immobilization and characterization of Fe (0) catalyst on NaOH-treated coal fly ash for catalytic reduction of p-nitrophenol. *Chemosphere*, 212, 1020-1029. <https://doi.org/10.1016/j.chemosphere.2018.09.006>.
14. Min, X., Han, C., Yang, L., & Zhou, C. (2021). Enhancing As (V) and As (III) adsorption performance of low alumina fly ash with ferric citrate modification: Role of FeSiO<sub>3</sub> and monosodium citrate. *Journal of Environmental Management*, 287, 112302. <https://doi.org/10.1016/j.jenvman.2021.112302>.

15. Mofulatsi, M., Prabakaran, E., Velepini, T., Green, E., & Pillay, K. (2022). Preparation of manganese oxide coated coal fly ash adsorbent for the removal of lead and reuse for latent fingerprint detection. *Microporous Mesoporous Materials*, 329, 111480. <https://doi.org/10.1016/j.micromeso.2021.111480>.
16. Nebaghe, K., El Boundati, Y., Ziat, K., Naji, A., Rghioui, L., & Saidi, M. (2016). Comparison of linear and non-linear method for determination of optimum equilibrium isotherm for adsorption of copper (II) onto treated Martil sand. *Fluid Phase Equilibria*, 430, 188-194. <https://doi.org/10.1016/j.fluid.2016.10.003>.
17. Oyehan, T.A., Olabemiwo, F.A., Tawabini, B.S., & Saleh, T.A. (2020). The capacity of mesoporous fly ash grafted with ultrathin film of polydiallyldimethyl ammonium for enhanced removal of phenol from aqueous solutions. *Journal of Cleaner Production*, 263, 121280. <https://doi.org/10.1016/j.jclepro.2020.121280>.
18. Pan, J., Li, L., Hang, H., Ou, H., Zhang, L., Yan, Y., & Shi, W. (2013). Study on the nonylphenol removal from aqueous solution using magnetic molecularly imprinted polymers based on fly-ash-cenospheres. *Chemical Engineering Journal*, 223, 824-832. <https://www.sciencedirect.com/science/article/pii/S1385894713001654#!>.
19. Park, J., & Bae, S. (2019). Highly efficient and magnetically recyclable Pd catalyst supported by iron-rich fly ash@ fly ash-derived SiO<sub>2</sub> for reduction of p-nitrophenol. *Journal of Hazardous Materials*, 371, 72-82. <https://doi.org/10.1016/j.jhazmat.2019.02.105>.
20. Park, J., Saratale, G.D., Cho, S.-K., Bae, S. (2020). Synergistic effect of Cu loading on Fe sites of fly ash for enhanced catalytic reduction of nitrophenol. *Science of the Total Environment*, 705, 134544. <https://doi.org/10.1016/j.scitotenv.2019.134544>.
21. Qi, L., Teng, F., Deng, X., Zhang, Y., & Zhong, X. (2019). Experimental study on adsorption of Hg (II) with microwave-assisted alkali-modified fly ash. *Powder Technology*, 351, 153-158. <https://doi.org/10.1016/j.powtec.2019.04.029>.
22. Rawat, M., & Bulasara, V.K. (2018). Synthesis and characterization of low-cost ceramic membranes from fly ash and kaolin for humic acid separation. *Korean Journal of Chemical Engineering*, 35, 725-733. <https://doi.org/10.1007/s11814-017-0316-6>.
23. Repo, E., 2011. EDTA-and DTPA-functionalized silica gel and chitosan adsorbents for the removal of heavy metals from aqueous solutions. Lappeenranta University of Technology Laboratory of Green Chemistry. <https://urn.fi/URN:ISBN:978-952-265-108-2>.
24. Shah, B.A., Pandya, D.D., & Shah, H.A. (2017). Impounding of ortho-chlorophenol by zeolitic materials adapted from bagasse fly ash: four factor three level Box-Behnken design modelling and optimization. *Arabian Journal for Science and Engineering*, 42, 241-260. <https://doi.org/10.1007/s13369-016-2294-0>.
25. Subbulekshmi, N., & Subramanian, E. (2017). Nano CuO immobilized fly ash zeolite Fenton-like catalyst for oxidative degradation of p-nitrophenol and p-nitroaniline. *Journal of Environmental Chemical Engineering*, 5, 1360-1371. <https://doi.org/10.1016/j.jece.2017.02.019>.
26. Tahari, N., Nefzi, H., Labidi, A., Ayadi, S., Abderrabba, M., & Labidi, J. (2021). Removal of Dyes and Heavy Metals with Clays and Diatomite, *Water Pollution and Remediation: Heavy Metals*. Springer, 539-569. [https://doi.org/10.1007/978-3-030-52421-0\\_16](https://doi.org/10.1007/978-3-030-52421-0_16).
27. Vu, D.-H., Bui, H.-B., Bui, X.-N., An-Nguyen, D., Le, Q.-T., Do, N.-H., & Nguyen, H. (2020). A novel approach in adsorption of heavy metal ions from aqueous solution using synthesized MCM-41 from coal bottom ash. *International Journal of Environmental Analytical Chemistry*, 100, 1226-1244. <https://doi.org/10.1080/03067319.2019.1651300>.
28. Wang, N., Hao, L., Chen, J., Zhao, Q., & Xu, H. (2018). Adsorptive removal of organics from aqueous phase by acid-activated coal fly ash: preparation, adsorption, and Fenton regenerative

- valorization of “spent” adsorbent. *Environmental Science and Pollution Research*, 25, 12481-12490. <https://doi.org/10.1007/s11356-018-1560-y>.
29. Wang, Y., Chen, B., Xiong, T., Zhang, Y., & Zhu, W. (2022). Immobilization of U (VI) in wastewater using coal fly ash aerogel (CFAA) as a low-cost adsorbent. *Process Safety and Environment Protection*, 160, 900-909. <https://doi.org/10.1016/j.psep.2022.03.006>.
  30. Yusof, M.S.M., Othman, M.H.D., Wahab, R.A., Samah, R.A., Kurniawan, T.A., Mustafa, A., Rahman, M.A., Jaafar, J., & Ismail, A.F. (2020). Effects of pre and post-ozonation on POFA hollow fibre ceramic adsorptive membrane for arsenic removal in water. *Journal of the Taiwan Institute of Chemical Engineers*, 110, 100-111. <https://doi.org/10.1016/j.jtice.2020.02.014>.
  31. Zhang, J., Yan, M., Sun, G., & Liu, K. (2021a). Simultaneous removal of Cu (II), Cd (II), Cr (VI), and rhodamine B in wastewater using TiO<sub>2</sub> nanofibers membrane loaded on porous fly ash ceramic support. *Separation and Purification Technology*, 272, 118888. <https://doi.org/10.1016/j.seppur.2021.118888>.
  32. Zhao, X., Zhao, H., Huang, X., Wang, L., Liu, F., Hu, X., Li, J., Zhang, G., & Ji, P. (2021). Effect and mechanisms of synthesis conditions on the cadmium adsorption capacity of modified fly ash. *Process Safety and Environment Protection*, 223, 112550. <https://doi.org/10.1016/j.ecoenv.2021.112550>.
  33. Zhu, L., Ji, J., Wang, S., Xu, C., Yang, K., & Xu, M. (2018). Removal of Pb (II) from wastewater using Al<sub>2</sub>O<sub>3</sub>-NaA zeolite composite hollow fiber membranes synthesized from solid waste coal fly ash. *Chemosphere*, 206, 278-284. <https://doi.org/10.1016/j.chemosphere.2018.05.001>.